Antigen delivery to early endosomes eliminates the superiority of human blood BDCA3$^+$ dendritic cells at cross presentation

Lillian Cohn,[1] Bithi Chatterjee,[1] Filipp Esselborn,[1] Anna Smed-Sörensen,[1,2] Norihiro Nakamura,[1] Cécile Chalouni,[1] Byoung-Chul Lee,[1] Richard Vandlen,[1] Tibor Keler,[3] Peter Lauer,[4] Dirk Brockstedt,[4] Ira Mellman,[1] and Lélia Delamarre[1]

[1]Genentech, South San Francisco, CA 94080
[2]Karolinska Institutet, 171 77 Solna, Sweden
[3]Celldex Therapeutics Inc., Phillipsburg, NJ 08865
[4]Aduro BioTech, Inc., Berkeley, CA 94710

Human BDCA3$^+$ dendritic cells (DCs), the proposed equivalent to mouse CD8α^+ DCs, are widely thought to cross present antigens on MHC class I (MHCI) molecules more efficiently than other DC populations. If true, it is unclear whether this reflects specialization for cross presentation or a generally enhanced ability to present antigens on MHCI. We compared presentation by BDCA3$^+$ DCs with BDCA1$^+$ DCs using a quantitative approach whereby antigens were targeted to distinct intracellular compartments by receptor-mediated internalization. As expected, BDCA3$^+$ DCs were superior at cross presentation of antigens delivered to late endosomes and lysosomes by uptake of anti-DEC205 antibody conjugated to antigen. This difference may reflect a greater efficiency of antigen escape from BDCA3$^+$ DC lysosomes. In contrast, if antigens were delivered to early endosomes through CD40 or CD11c, BDCA1$^+$ DCs were as efficient at cross presentation as BDCA3$^+$ DCs. Because BDCA3$^+$ DCs and BDCA1$^+$ DCs were also equivalent at presenting peptides and endogenously synthesized antigens, BDCA3$^+$ DCs are not likely to possess mechanisms for cross presentation that are specific to this subset. Thus, multiple DC populations may be comparably effective at presenting exogenous antigens to CD8$^+$ T cells as long as the antigen is delivered to early endocytic compartments.

CORRESPONDENCE
Lélia Delamarre:
delamarre.lelia@gene.com

Abbreviations used: IAV, influenza A virus; KBMA, killed but metabolically active; LLO, listeriolysin O; mDC, myeloid DC; MFI, mean fluorescence intensity; mo-DC, monocyte-derived DC; pDC, plasmacytoid DC; PFA, paraformaldehyde; ROS, reactive oxygen species.

DCs play a central role in initiating antigen-specific immunity and tolerance (Banchereau and Steinman, 1998; Lanzavecchia and Sallusto, 2001; Joffre et al., 2009). They are a heterogeneous population of antigen-presenting cells that differ in their tissue distribution, surface expression markers, and function (Heath and Carbone, 2009). DCs can be divided into two major subsets: plasmacytoid DCs (pDCs) and myeloid DCs (mDCs, also called conventional DCs). pDCs play a crucial role in providing protection against viruses by producing significant amounts of type I interferon upon engagement of TLR7 and 9 (Villadangos and Young, 2008, Cervantes-Barragan et al., 2012) and intracellular sensors (Hornung et al., 2004; Kumagai et al., 2009).

mDCs are known for their ability to capture and present antigens to T cells, promoting tolerance under steady-state conditions and immunity upon encounter of proinflammatory molecules. Splenic mDCs have been extensively studied in mice and can be divided into two major subsets based on surface expression of CD11b or CD8α. Importantly, these subsets have specialized functions (Heath and Carbone, 2009). Although CD11b$^+$CD8α$^-$ mDCs are potent at presenting MHC class II (MHCII)–bound peptides to CD4$^+$ T cells, CD8α$^+$ DCs are widely thought to exhibit an enhanced capacity for antigen cross presentation: the ability to load exogenous antigen onto MHCI for the priming of CD8$^+$ T cells responses (Dudziak

© 2013 Cohn et al. This article is distributed under the terms of an Attribution–Noncommercial–Share Alike–No Mirror Sites license for the first six months after the publication date (see http://www.rupress.org/terms). After six months it is available under a Creative Commons License (Attribution–Noncommercial–Share Alike 3.0 Unported license, as described at http://creativecommons.org/licenses/by-nc-sa/3.0/).

The Rockefeller University Press $30.00
J. Exp. Med. 2013 Vol. 210 No. 5 1049-1063
www.jem.org/cgi/doi/10.1084/jem.20121251

The Journal of Experimental Medicine

Downloaded from http://rupress.org/jem/article-pdf/210/5/1049/1748340/jem_20121251.pdf by guest on 09 February 2026

et al., 2007; Shortman and Heath, 2010). Indeed, the genetic deletion of the Batf3 transcription factor leads to the loss of the CD8α$^+$ DC subset in mice (Hildner et al., 2008). DCs from Batf3$^{-/-}$ mice are defective at antigen cross presentation in vitro as well as viral and tumor immunity in vivo.

The molecular mechanisms underlying the role of CD8α$^+$ DCs in antigen cross presentation are not yet fully understood (Amigorena and Savina, 2010; Segura and Villadangos, 2011). As previously found for presentation of exogenous antigens on MHCII (Trombetta and Mellman, 2005), increased cross presentation efficiency at least partly reflects a reduced ability to degrade internalized antigens as a result of low protease expression and regulation of ATP-driven acidification in lysosomes. An additional mechanism specific to CD8α$^+$ DCs is the ability to generate reactive oxygen species (ROS) via NOX-2 activation that further reduces proteolysis and enhances cross presentation by elevating lysosomal pH and directly inactivating cysteine proteases (Savina et al., 2006, 2009; Rybicka et al., 2012).

Limited lysosomal or phagosomal proteolysis presumably favors cross presentation by preserving internalized antigens long enough for them to be exported to the cytosol, enabling proteasomal proteolysis and subsequent peptide translocation by the TAP-1/2 peptide transporter into the ER, or back to endocytic compartments, for loading on MHCI (Cebrian et al., 2011). This possibility is supported by observations showing that inhibition of lysosomal protease activity increases cross presentation on MHCI (Accapezzato et al., 2005; Belizaire and Unanue, 2009; Chatterjee et al., 2012). Targeting antigen to early endosomes leads to efficient cross presentation, possibly as a result of the limited degradative capacity of this compartment, although quantitative comparisons have generally not been possible (Burgdorf et al., 2007; Peng and Elkon, 2011; Tacken et al., 2011; Zelenay et al., 2012) until recently (Chatterjee et al., 2012).

Recent studies of mouse DCs have raised some questions, however, regarding the degree to which CD8α$^+$ DCs are specialized for antigen cross presentation. One possibility is that the amount or route of antigen uptake is a major factor, such that CD8α$^+$ DCs appear superior when antigen is internalized by fluid phase endocytosis or phagocytosis but not after receptor-mediated endocytosis via DEC205 (Kamphorst et al., 2010). Thus, it is unclear whether there are fundamental mechanistic differences between DC subsets, or if their differences in function are context dependent, or both.

Understanding cross presentation in human DCs is more problematic because detailed study has been limited as a result of the difficulty in isolating sufficient numbers of DCs for experimental work. Gene expression profiling has suggested that human CD141$^+$/BDCA3$^+$ DCs are the functional equivalent of the mouse CD8α$^+$ DCs, whereas human CD1c$^+$/BDCA1$^+$ DCs resemble mouse CD11b$^+$CD8α$^-$ DCs (Robbins et al., 2008; Crozat et al., 2010b). Human BDCA3$^+$ DCs, mouse CD8α$^+$ DCs, and the closely related mouse CD103$^+$ DCs are the only DC subsets to express DNGR1, a receptor for necrotic cells (also called Clec9a); both BDCA3$^+$ DCs and CD8α$^+$ DCs express the accessory molecules XCR1 and NECL2 (Crozat et al., 2010a; Poulin et al., 2010, 2012). Importantly, BDCA3$^+$ DCs are potent at inducing CD8$^+$ T cell responses in vitro, although their superiority to other human DC subsets is unclear (Bachem et al., 2010; Crozat et al., 2010a; Jongbloed et al., 2010; Poulin et al., 2010; Mittag et al., 2011; van de Ven et al., 2011; Segura et al., 2012).

We recently found that the efficiency of cross presentation of receptor-targeted antigens by BDCA1$^+$ DCs and monocyte-derived DCs (mo-DCs) is largely determined by the endocytic compartments to which the antigen was delivered, with delivery to early endosomes being far superior (Chatterjee et al., 2012). To determine whether differences in intracellular trafficking might also influence the relative capacities of BDCA3$^+$ DCs and BDCA1$^+$ DCs for cross presentation, we developed optimized protocols to isolate DCs from human blood in sufficient quantities and purity to facilitate detailed biochemical and functional characterization of these cells. We find that BDCA3$^+$ DCs are superior to BDCA1$^+$ DCs for cross presenting antigen targeted to late endosomes and lysosomes, suggesting that BDCA3$^+$ DCs may have enhanced antigen escape from this compartment. In contrast, antigen targeting to early endosomes equalizes the relative capacities for cross presentation between these two cell types.

RESULTS

Isolated BDCA3$^+$ DCs from human blood are more mature than BDCA1$^+$ DCs

A major limitation to studying primary human DCs, especially BDCA3$^+$ DCs, is their scarcity in human tissues and blood (<0.1% of PBMCs; Dzionek et al., 2000). We therefore developed an isolation scheme optimized to obtain the three major blood DC subsets with high yield and purity. PBMCs were collected from healthy donors by automated leukapheresis, and enriched populations of lymphocytes, monocytes, and DCs were obtained by counterflow elutriation. BDCA1$^+$ DCs, because of their relative abundance, were isolated from one third of the monocyte/DC fraction by positive immunomagnetic selection using the anti-BDCA1 mAb clone AD5-8E7 (Smed-Sörensen et al., 2005). pDCs and BDCA3$^+$ DCs were isolated sequentially from the remaining two thirds with the same approach using mAb clones AD5-17F6 and AD5-14H12, respectively. Before isolation, the monocyte/DC fraction contained primarily CD14$^+$ monocytes and ∼2% BDCA1$^+$ DCs, 0.5% pDCs, and 0.2% BDCA3$^+$ DCs; after isolation, the three populations were highly enriched in DCs (up to 95%). The BDCA1$^+$ DC and BDCA3$^+$ DC populations on average contained 10% CD14$^+$ monocytes, whereas the pDC-enriched population contained <5% CD14$^+$ monocytes (Fig. 1, A–D). For functional experiments, only populations with >75% purity were used. Typical yields per donor were 5–20 × 10^6 BDCA1$^+$ DCs, 2–8 × 10^6 pDCs, and 1–3 × 10^6 BDCA3$^+$ DCs.

After overnight culture in the absence of TLR agonists, BDCA3$^+$ DCs displayed a more mature phenotype than BDCA1$^+$ DCs, with elevated levels of surface MHCI, MHCII,

Downloaded from http://rupress.org/jem/article-pdf/210/5/1049/1748340/jem_20121251.pdf by guest on 09 February 2026

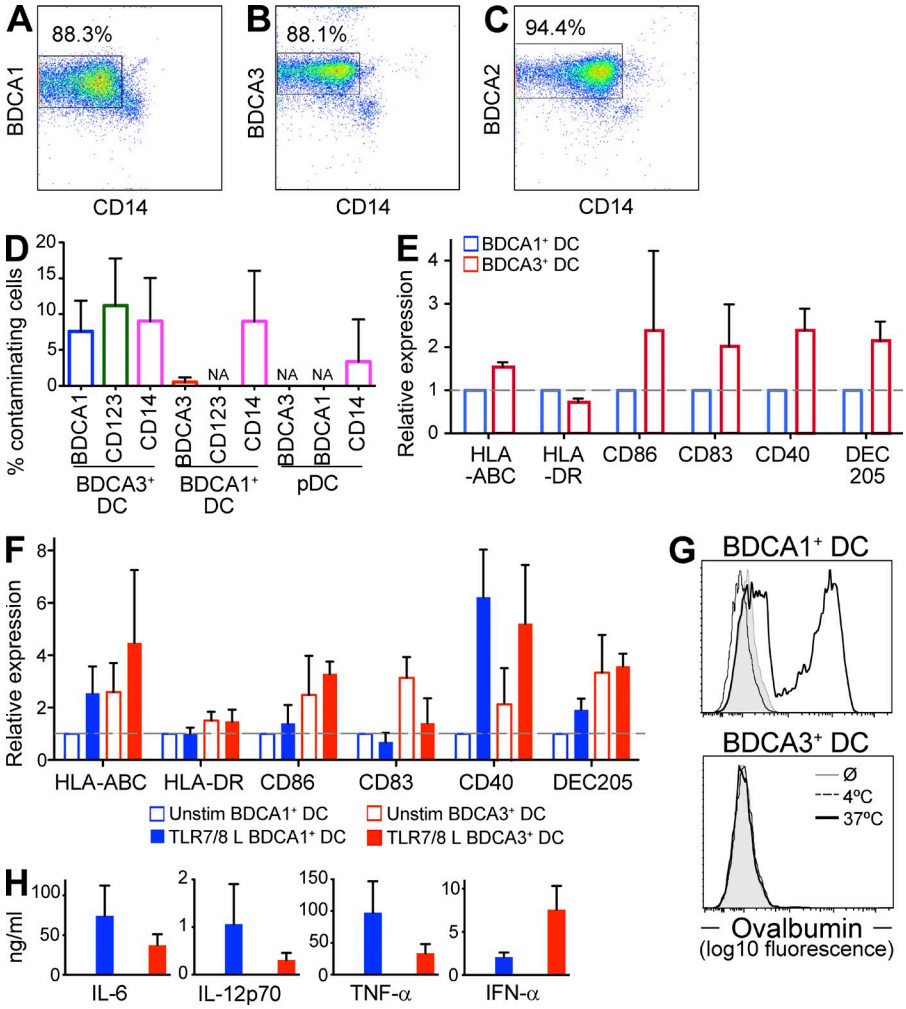

Figure 1. BDCA3+ DCs have a more mature phenotype than BDCA1+ DCs. (A–C) Shown are representative plots for BDCA1+ DCs (A), BDCA3+ DCs (B), and pDCs (C) after isolation (representative of $n > 20$ donors). (D) Percentage of contaminating cells in isolated DC subsets. Isolated DC fractions were labeled for contaminating cell subsets with antibodies against CD14, CD123, BDCA1, or BDCA3. Live cells were gated on the above markers and the percentage of contaminating subsets was determined. Data are the mean ± SD ($n = 7$ independent experiments). NA, not applicable (below limit of detection). (E) Phenotype of DC subsets in freshly isolated PBMCs. DCs in PBMCs were labeled for the indicated markers and analyzed by flow cytometry. Isotype background fluorescence was subtracted from the mean fluorescence intensity (MFI), and MFI was normalized to unstimulated BDCA1+ DCs. Data are the mean ± SD ($n = 6$ independent experiments). (F) Phenotype of isolated DC subsets after overnight culture in the presence or absence of TLR7/8 L. After overnight culture, DCs were labeled for the indicated markers and analyzed by flow cytometry. Isotype background fluorescence was subtracted from the MFI, and MFI was normalized to unstimulated BDCA1+ DCs. Data are the mean ± SD ($n = 6$ independent experiments). (G) Endocytic capacity of isolated DC subsets. Overnight cultured isolated DCs were pulsed with 5 µg/ml Alexa Fluor 488 ovalbumin for 20 min at 37 or 4°C, and ovalbumin uptake was analyzed by flow cytometry. Shown is one representative experiment of three. (H) Cytokine production by isolated DC subsets after overnight culture in the presence or absence of TLR7/8 L. Supernatants were collected and analyzed for indicated cytokine production by Luminex. Data are the mean ± SD ($n = 3$ independent experiments).

CD86, CD83, CD40, and DEC205 (Fig. 1 F). This is in agreement with previous observations (Jongbloed et al., 2010). Also similar to mature DCs, the unstimulated BDCA3+ DCs exhibited a decreased capacity to take up ovalbumin by fluid phase endocytosis (Garrett et al., 2000; Fig. 1 G). This phenotype was not the result of the isolation procedure; BDCA3+ DCs from freshly isolated PBMCs also exhibited a more mature phenotype than BDCA1+ DCs (Fig. 1 E).

Although they exhibited some of the hallmarks of mature DCs, unstimulated BDCA3+ DCs did not produce inflammatory cytokines, suggesting that they were phenotypically but not functionally mature (Jiang et al., 2007; Fig. 1 H). After stimulation with a TLR7/8 agonist (TLR7/8 L), however, BDCA3+ DCs not only further up-regulated some surface markers (e.g., CD40; Fig. 1 F) but also produced inflammatory cytokines (Fig. 1 H). BDCA3+ DCs produced higher levels of IFN-α than BDCA1+ DCs, as previously described (Jongbloed et al., 2010), but produced similar or lower levels of IL-12p70. This was in contrast to published data that BDCA3+ DCs were the only subset able to produce IL-12, albeit in response to the TLR3 agonist poly(I:C) (Jongbloed et al., 2010). In any case, after induction of maturation, BDCA3+ DCs did not differ dramatically from BDCA1+ DCs with respect to surface marker expression or cytokine production.

BDCA3+ DCs and BDCA1+ DCs have similar capacities to present endogenous antigen on MHCI

We compared the capacity of BDCA3+ DCs and BDCA1+ DCs to present peptide antigen to autologous CD8+ T cells. We used the Flu-M1 (aa 58–66) epitope as a model antigen and screened HLA-A*0201 donors for preexisting CD8+ T cell responses against this epitope. Unstimulated BDCA1+ and BDCA3+ DCs from HLA-A*0201 donors were incubated with preprocessed Flu-M1 (aa 58–66) peptide and assayed over a range of DC/T cell ratios (Fig. 2 A) and peptide concentrations (not depicted). Both DC subsets induced similar

Downloaded from http://rupress.org/jem/article-pdf/210/5/1049/1748340/jem_20121251.pdf by guest on 09 February 2026

Flu-M1–specific CD8+ T cell proliferation. Thus, BDCA3+ DCs do not have an inherently greater ability to stimulate CD8+ T cells in vitro.

We next examined the capacity of the human blood DC subsets to process and present endogenous antigen on MHCI. DCs were transfected with a construct that encoded a Flu-M1 (aa 55–72)-EGFP fusion protein expressed in the cytosol. After overnight culture in the presence or absence of TLR7/8 L, we monitored EGFP expression by flow cytometry and found that EGFP expression levels of the transfected cells were similar between BDCA1+ DCs and BDCA3+ DCs (Fig. 2 B). BDCA3+ DCs and BDCA1+ DCs exhibited little difference in their ability to present endogenous Flu-M1 on MHCI (Fig. 2 C). This was true regardless of whether DCs were immature (unstimulated: Fig. 2 C, left) or mature (TLR7/8 L stimulated: Fig. 2 C, right). These data indicate that the overall efficiency of the endogenous MHCI presentation machinery is similar between the two DC subsets.

BDCA3+ DCs exhibit increased cross presentation of antigen delivered to late endosomes and lysosomes via DEC205

Recent work has demonstrated that human BDCA3+ DCs have the capacity to cross present antigens (Bachem et al., 2010; Crozat et al., 2010a; Jongbloed et al., 2010; Poulin et al., 2010; Mittag et al., 2011; van de Ven et al., 2011; Segura et al., 2012). However, their superiority in comparison with other DCs is unclear. A limitation is that most of these previous studies did not quantify the amount or characterize the route of antigen uptake by DCs. To address this problem, we used antibodies to deliver quantifiable amounts of antigen to both BDCA3+ DCs and BDCA1+ DCs, allowing determinations of cross presentation efficiency as a function of antigen uptake.

We first allowed DCs to internalize an anti-DEC205 antibody covalently conjugated to an extended Flu-M1 peptide (aa 55–72; Chatterjee et al., 2012) and then determined cross presentation by measuring Flu-M1–specific CD8+ T cell proliferation. Strikingly, BDCA3+ DCs cross presented DEC205-targeted Flu-M1 far more efficiently than BDCA1+ DCs. BDCA1+ DCs seldom generated a detectable CD8+ T cell response to Flu-M1 peptide antigen targeted through DEC205 (Fig. 3 A). Similar data were obtained using anti-DEC205 antibody conjugated to a CMV-pp65 peptide, although in this case some cross presentation by BDCA1+ DCs was observed, especially in the presence of TLR7/8 L (Fig. 3 B).

We next asked whether the enhanced cross presentation by BDCA3+ DCs reflected an increase in antigen uptake. Using a fluorescently labeled anti-DEC205 antibody, BDCA1+ DCs and BDCA3+ DCs were allowed to internalize antibody for 4–6 h and antibody accumulation was then determined by flow cytometry. Anti-DEC205 antibodies accumulated similarly in BDCA3+ DCs and BDCA1+ DCs (Fig. 3 C), despite the higher surface levels of DEC205 on BDCA3+ DCs

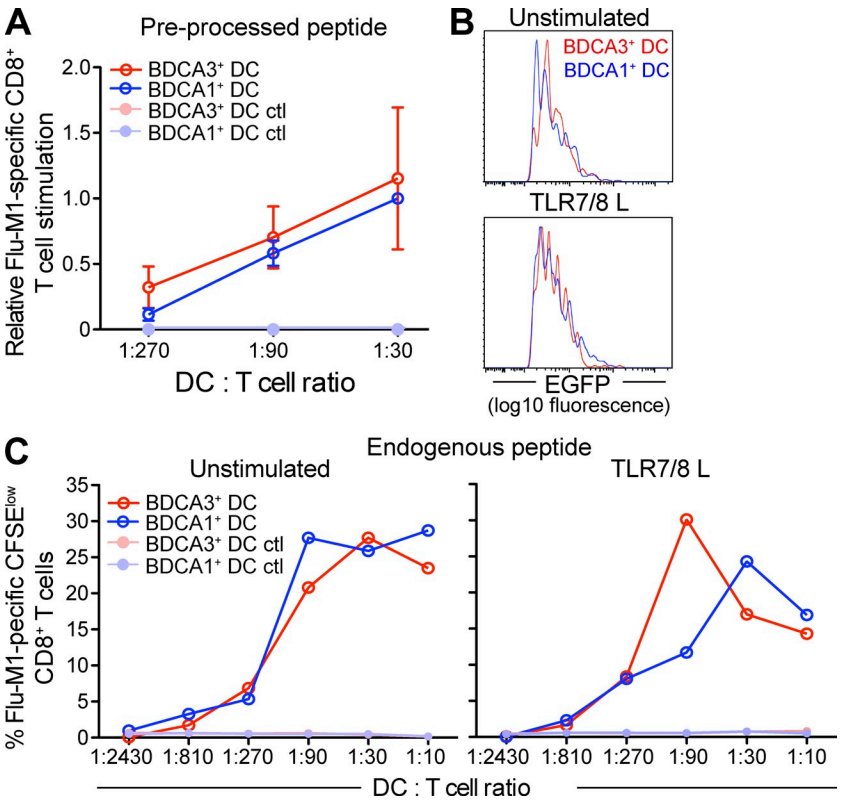

Figure 2. BDCA3+ DCs and BDCA1+ DCs have a similar ability to present endogenous antigen on MHCI. (A) Presentation of preprocessed peptide by DCs. Day 1 DCs from HLA-A*0201 donors were incubated with Flu-M1 (aa 58–66) or HIV-p17 (aa 77–85, negative control) peptide at 25 ng/ml for 3 h at 37°C. The cells were then washed and cultured with autologous CFSE-labeled CD8+ T cells at indicated DC/T cell ratio in the presence of TLR7/8 L. 8–10 d later, Flu-M1–specific CD8+ T cell expansion was evaluated by gating on CFSElow cells positive for Flu-M1 (aa 58–66) pentamer. Shown data are normalized to BDCA1+ DC/T cells at a 1:30 ratio and the mean ± SD (n = 4 independent experiments) is depicted. (B) EGFP fluorescence intensity in DC subsets. DCs from HLA-A*0201 donors were transfected directly after isolation with a plasmid encoding for Flu-M1 (aa 55–72)–EGFP fusion protein. DCs were cultured overnight in the presence or absence of TLR7/8 L. 16 h after transfection, DCs were analyzed by flow cytometry for the expression of EGFP. Shown histograms are DCs gated on live EGFP+ cells. Shown is one representative experiment of three. (C) Presentation of endogenous antigen by DCs. Flu-M1 (aa 55–72)-EGFP–transfected DCs were cultured overnight in the presence or absence of TLR7/8 L and then cultured with autologous CFSE-labeled CD8+ T cells at indicated DC/T cell ratios, normalized to percentage of EGFP+ DCs. 8–10 d later, Flu-M1–specific CD8+ T cell expansion was evaluated as in A. Shown is one representative experiment of three.

Downloaded from http://rupress.org/jem/article-pdf/210/5/1049/1748340/jem_20121251.pdf by guest on 09 February 2026

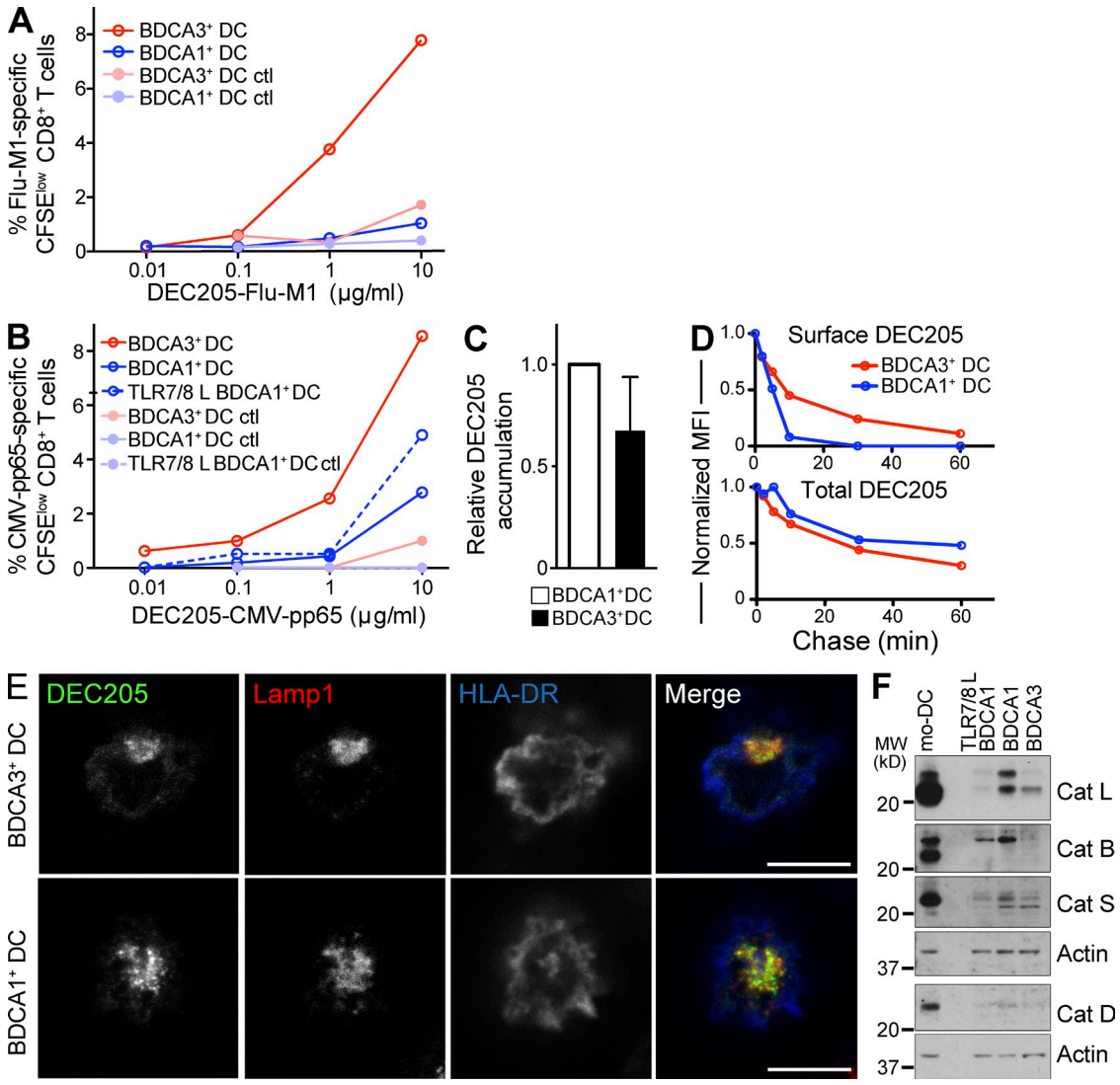

Figure 3. BDCA3+ DC exhibit an enhanced ability to cross present antigen delivered to lysosomes. (A) Antigen cross presentation via DEC205 by BDCA3+ DCs and BDCA1+ DCs. Day 1 DCs from HLA-A*0201 donors were fed with anti-DEC205 or control isotype antibody conjugated to Flu-M1 (aa 55–72) at the indicated doses for 4 h at 37°C. The cells were then washed and cultured with autologous CFSE-labeled CD8+ T cells in the presence of IL-2 and TLR7/8 L. 8–10 d later, Flu-M1–specific CD8+ T cell expansion was evaluated by gating on CFSE^{low} cells positive for Flu-M1 (aa 58–66) pentamer. Shown is one representative experiment of $n > 6$. (B) As in A; anti-DEC205 and the control isotype antibodies were conjugated to CMV-pp65 (aa 488–508). Shown is one representative experiment of two. (C) Accumulation of anti-DEC205 antibody. Day 1 DCs were fed with Alexa Fluor 488–labeled anti-DEC205 antibody continuously for 4–6 h at 4 or 37°C. Results were analyzed by flow cytometry. 4°C MFI was subtracted from the 37°C MFI, and the resulting MFI was normalized to BDCA1+ DCs. Data shown are the mean MFI ± SD ($n = 7$ independent experiments). (D) Internalization of anti-DEC205 antibody. Day 1 DCs were incubated with Alexa Fluor 488–labeled anti-DEC205 antibody for 30 min at 4°C. The cells were then washed and cultured at 37°C for the indicated times. At each time point, cells were labeled with an Alexa Fluor 647–labeled anti–human IgG antibody to label remaining surface bound antibody. Cells were then analyzed by flow cytometry. The total DEC205 is Alexa Fluor 488–labeled antibody, whereas the surface DEC205 is the Alexa Fluor 647–labeled anti–human antibody. Shown is one representative experiment of four. (E) Anti-DEC205 antibody trafficking. Day 1 DCs were fed Alexa Fluor 488–labeled anti-DEC205 antibody (green) continuously for 3 h at 37°C, washed, and allowed to adhere to coverslips. After fixation and permeabilization, the lysosomes and cell membrane were stained using anti-Lamp1 (red) and anti–HLA-DR (blue) antibodies, respectively. Cells were then analyzed using confocal microscopy. Bars, 7.5 µm. Shown is one representative experiment of five. (F) Detection of the indicated lysosomal proteases by Western blot of day 1 BDCA1+ DCs, BDCA3+ DCs, and mo-DCs. DC subsets were lysed and analyzed by Western blot for lysosomal protease expression. Shown is one representative experiment of three.

(Fig. 1 F). Next, we compared the kinetics of internalization of DEC205 in these two DC subsets (Fig. 3 D). We found that BDCA3+ DCs internalized DEC205 far more slowly than BDCA1+ DCs; BDCA3+ DCs demonstrated an almost complete disappearance of surface anti-DEC205 antibody after a 60-min chase, whereas >90% of anti-DEC205 antibody

Downloaded from http://rupress.org/jem/article-pdf/210/5/1049/1748340/jem_20121251.pdf by guest on 09 February 2026

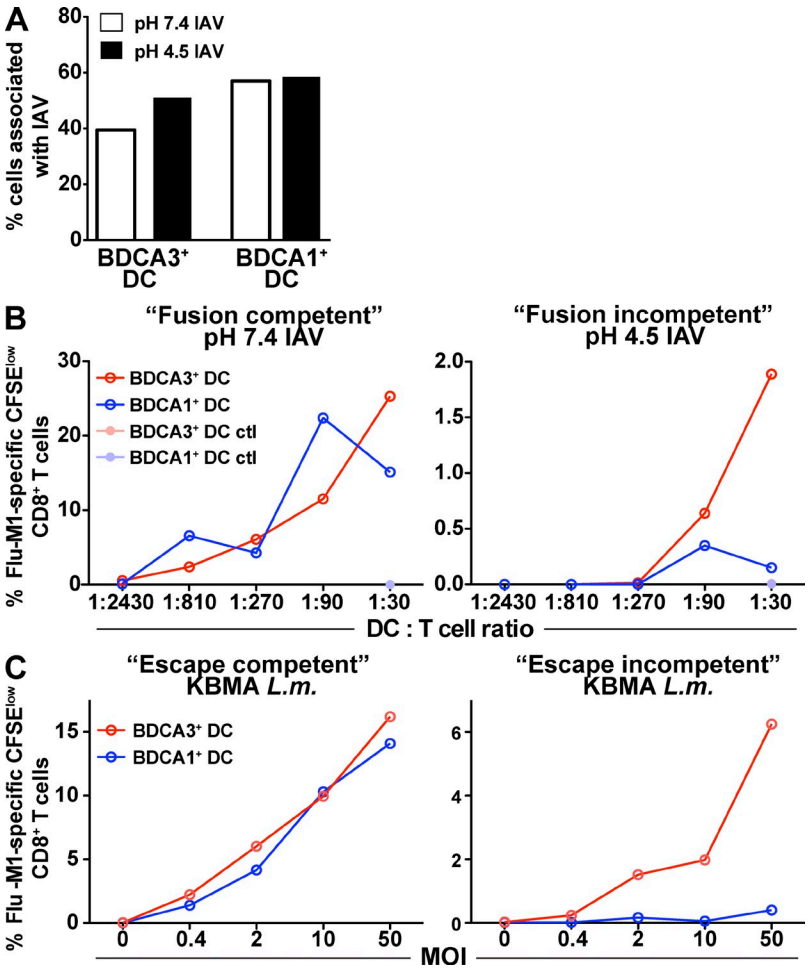

Figure 4. Antigens escaping from lysosomes are cross presented equally by both DC subsets. (A) Number of IAV particles associated with DCs. Day 1 DCs were fed either with fusion-competent or -incompetent replication-defective (heat inactivated, HI) IAV for 6 h at 37°C. The cells were then washed and allowed to adhere to coverslips. After fixation and permeabilization, the cells were labeled with an anti-NP antibody. Cells were analyzed by confocal microscopy. Numbers of cells associated with IAV particles were counted and quantified. Shown is one representative experiment of three. (B) Cross presentation of fusion-competent and fusion-incompetent HI IAV. Day 1 DCs from HLA-A*0201 donors were fed with fusion-competent pH 7.4–treated HI IAV or fusion-incompetent pH 4.5–treated HI IAV for 6 h at 37°C. The cells were then washed and cultured with autologous CFSE-labeled $CD8^+$ T cells. 8–10 d later, $CD8^+$ T cell expansion was evaluated by gating on $CFSE^{low}$ cells positive for Flu-M1 (aa 58–66) pentamer. Shown is one representative experiment of three. (C) Cross presentation of escape-competent and escape-incompetent KBMA *L. monocytogenes*. Day 1 DCs from HLA-A*0201 donors were fed for 1 h with escape-incompetent (LLO^-) and escape-competent (LLO^+) KBMA *L. monocytogenes* strains engineered to secrete ActAN100-Flu-M1 (aa 58–66) fusion protein. The cells were then washed and, as in B, cultured with autologous T cells to measure antigen cross presentation. Shown is one representative experiment of three.

was internalized within 10 min in $BDCA1^+$ DCs. In addition, the internalized anti-DEC205 antibodies were delivered to Lamp1-positive late endosomes and lysosomes in both DC types (Fig. 3 E). Collectively, these results indicate that $BDCA3^+$ DCs were not superior at cross presentation via DEC205 because they internalized more antigen or because they delivered internalized antigen to a distinct intracellular destination relative to $BDCA1^+$ DCs.

Superiority in cross presentation has been suggested to be caused, at least in part, by the reduced ability of the cells to degrade antigens in their endocytic compartments (Savina et al., 2006, 2009; Mantegazza et al., 2008). We therefore examined the levels of lysosomal proteases present in $BDCA1^+$ and $BDCA3^+$ DC subsets by Western blot analysis. The levels of precursor and active cathepsins B, D, L, and S were slightly decreased in $BDCA3^+$ DCs in comparison with immature $BDCA1^+$ DCs (Fig. 3 F). However, TLR7/8 L stimulation reduced cathepsin expression by $BDCA1^+$ DCs to levels at least as low as in $BDCA3^+$ DCs. The rates of anti-DEC205 antibody degradation were also not discernibly different between the two cell types (unpublished data). Thus, although $BDCA3^+$ DCs appeared more efficient at cross presenting extended peptide antigens selectively delivered to lysosomal compartments, this difference could not be easily attributed to differences in lysosomal proteolytic potential between the two cell types.

Enhancing antigen escape from late endosomes and lysosomes equalizes the cross presentation efficiency of $BDCA1^+$ DCs and $BDCA3^+$ DCs

A likely rate-limiting step in cross presentation is the egress of internalized antigen from endocytic compartments to the cytosol, an event which requires passage through a compartment barrier normally impermeable to macromolecules. Because the mechanism of antigen egress is unknown, we devised an approach to ask if $BDCA3^+$ DCs might conduct this step more efficiently, thereby mediating more efficient cross presentation. For this purpose, we used the pH-based fusion properties of Influenza A virus (IAV), which normally infects host cells by releasing its nucleocapsid into the cytosol after the hemagglutinin-mediated fusion of the viral envelope with the limiting membrane of endosomes (Stegmann et al., 1989). IAV enters the cytosol via late endosomes and lysosomes because its fusion pH optimum is less than pH 5.2. Pretreatment of IAV with a low pH buffer renders the virus irreversibly unable to fuse with the endosomal membrane

Downloaded from http://rupress.org/jem/article-pdf/210/5/1049/1748340/jem_20121251.pdf by guest on 09 February 2026

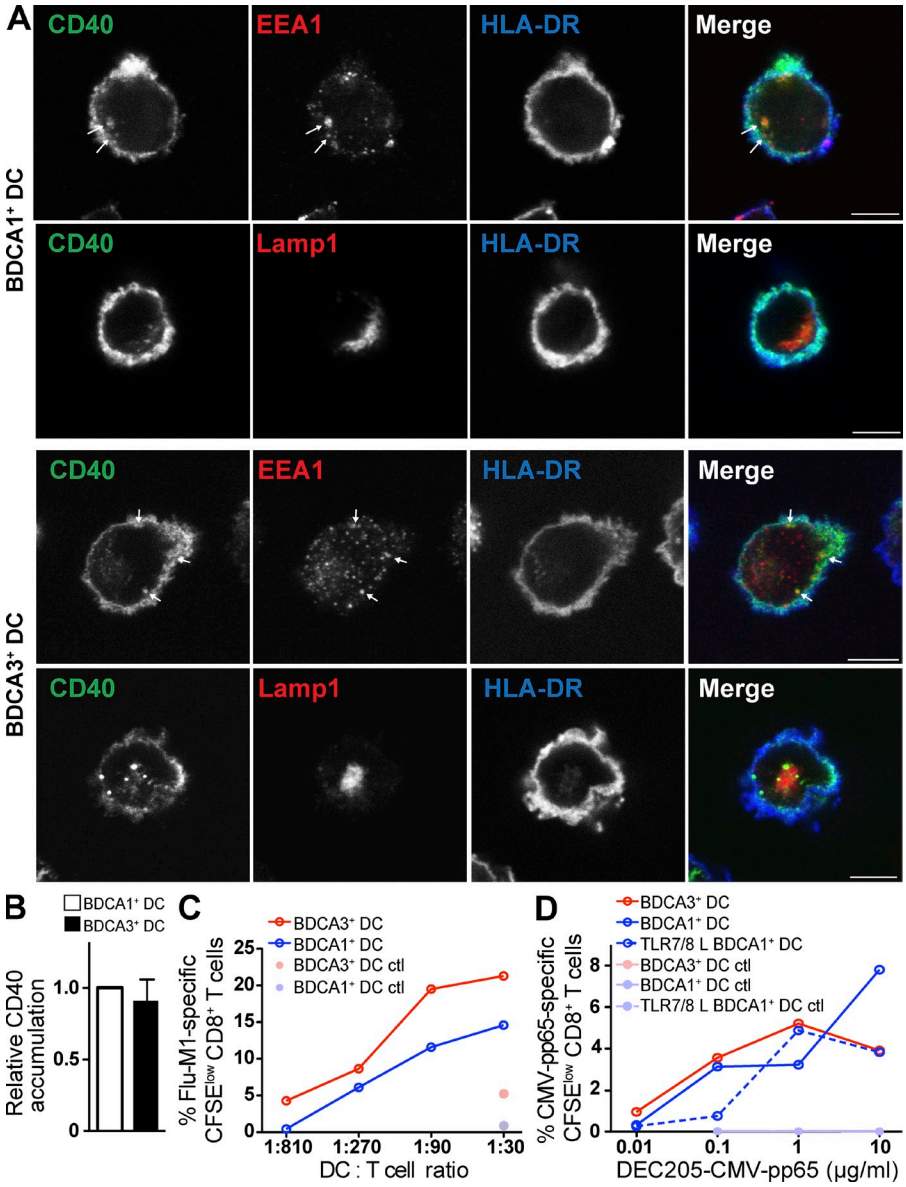

Figure 5. Antigen targeted to early endosomes via CD40 is cross presented by both DC subsets with similar efficacy. (A) Anti-CD40 antibody intracellular trafficking. Day 1 BDCA1+ DCs (top) or BDCA3+ DCs (bottom) were fed with Alexa Fluor 488–labeled anti-CD40 antibody (green) continuously for 3 h at 37°C, washed, and allowed to adhere to coverslips. After fixation and permeabilization, the lysosomes or early endosomes were stained using anti-Lamp1 or anti-EEA1 (red), respectively. Plasma membrane was stained using anti–HLA-DR (blue) antibodies. Cells were then analyzed using confocal microscopy. Bars, 5 µm. Shown is one representative experiment of three. (B) Accumulation of anti-CD40 antibody. Day 1 DCs were fed with Alexa Fluor 488–labeled anti-CD40 antibody continuously for 4–6 h at 4°C or 37°C. Results were analyzed by flow cytometry. The 4°C MFI was subtracted from the 37°C MFI, and the resulting MFI was normalized to BDCA1+ DCs. Data shown are the mean MFI ± SD ($n = 3$ independent experiments). (C) Antigen cross presentation via CD40 in DC subsets. Day 1 isolated DCs from HLA-A*0201 donors were fed with anti-CD40, or control isotype antibody conjugated to Flu-M1 (aa 55–72) at 1 µg/ml for 4 h at 37°C. The cells were then washed and cultured with autologous CFSE-labeled CD8+ T cells in the presence of IL-2 and TLR7/8 L. 8–10 d later, Flu-M1–specific CD8+ T cell expansion was evaluated by gating on $CFSE^{low}$ cells positive for Flu-M1 (aa 58–66) pentamer. Shown is one representative experiment of more than five. (D) As in C; anti-CD40 and control isotype antibodies were conjugated to CMV-pp65 (aa 488–508) at the indicated doses. Shown is one representative experiment of two.

(Stegmann et al., 1987). In our system, this differential viral fusion provides antigen (Flu-M1 protein) in a form that either can or cannot be efficiently translocated to the cytosol.

Fusion-competent (pH 7.4 pretreated) virus or fusion-incompetent (pH 4.5 pretreated) virions were added to BDCA1+ DCs and BDCA3+ DCs for 6 h to allow virus endocytosis. Both cell types were found to associate with comparable amounts of both types of virus by counting virus particles by immunofluorescence microscopy (Fig. 4 A). We next measured cross presentation of Flu-M1. Flu-M1 protein from fusion incompetent virus was cross presented far more efficiently by BDCA3+ DCs than by BDCA1+ DCs (Fig. 4 B, right), in agreement with the DEC205-Flu-M1 peptide-targeting experiments. In contrast, Flu-M1 protein from fusion-competent virus was presented equivalently by both DC populations (Fig. 4 B, left).

Similar results were obtained with killed but metabolically active (KBMA) *Listeria monocytogenes* engineered to express Flu-M1 (aa 58–66) epitope as an antigen delivery vehicle (Skoberne et al., 2008; Fig. 4 C). Delivery of Flu-M1 peptide expressing KBMA *L. monocytogenes*, which actively gains access to the cytosol through expression of listeriolysin O (LLO), resulted in similar MHCI presentation by BDCA1+ DCs and BDCA3+ DCs (Fig. 4 C, left). Conversely, Flu-M1 peptide expressed by LLO-deficient KBMA *L. monocytogenes*, which is incapable of escaping the phagosome, resulted in more efficient cross presentation by BDCA3+ DCs (Fig. 4 C, right).

Together, these data indicate that once the antigen has reached the cytosol, it accesses the MHCI pathway with the same efficiency in both BDCA1+ DCs and BDCA3+ DCs. In addition, BDCA3+ DCs appear to differ from BDCA1+ DCs either at the step of antigen translocation into the cytosol or

Downloaded from http://rupress.org/jem/article-pdf/210/5/1049/1748340/jem_20121251.pdf by guest on 09 February 2026

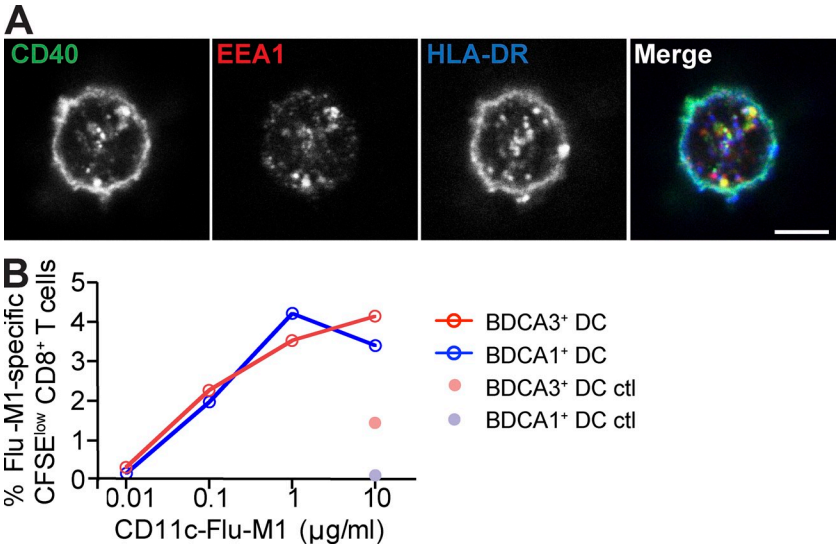

Figure 6. Antigen targeted to early endosomes via CD11c is cross presented by both DC subsets with similar efficacy. (A) Anti-CD11c antibody intracellular trafficking. Day 1 BDCA1$^+$ DCs were fed with Alexa Fluor 488–labeled anti-CD11c antibody (green) continuously for 3 h, washed, and allowed to adhere to coverslips. After fixation and permeabilization, the early endosomes and plasma membrane were stained using EEA1 (red) and anti–HLA-DR (blue) antibodies, respectively. Cells were then analyzed using confocal microscopy. Bar, 5 µm. Shown is one representative experiment of three. (B) Antigen cross presentation via CD11c in DC subsets. Day 1 isolated DCs from HLA-A*0201 donors were fed with anti-CD11c or control isotype antibody conjugated to Flu-M1 (aa 55–72) at indicated doses for 4 h at 37°C. The cells were then washed and cultured with autologous CFSE-labeled CD8$^+$ T cells in the presence of IL-2 and TLR7/8 L. 8–10 d later, CD8$^+$ T cell expansion was evaluated by gating on CFSE^{low} cells positive for Flu-M1 (aa 58–66) pentamer. Shown is one representative experiment of three.

at a step upstream of it within the endocytic system. It is also noteworthy that the fusion-competent virus is more efficiently cross presented by BDCA3$^+$ DCs than the fusion-incompetent virus (25 vs. 2% proliferating Flu-M1–specific CD8$^+$ T cells; Fig. 4 B). Collectively, these results strongly suggest that a potential rate-limiting step in the cross presentation pathway is at the level of antigen egress from late endosomes and lysosomes. It appears that BDCA3$^+$ DCs are able to navigate this step more effectively than BDCA1$^+$ DCs.

Targeting an early endosomal compartment results in efficient cross presentation by both BDCA3$^+$ DCs and BDCA1$^+$ DCs

Our data indicate that the late endosomal/lysosomal compartment of BDCA3$^+$ DCs may uniquely support cross presentation by allowing increased antigen access to the cytosol, either by subtly limiting antigen degradation in lysosomes or by providing antigen from a more rapid mechanism of escape. To determine whether this unique compartmental capacity for cross presentation applies to other endosomal compartments in BDCA3$^+$ DCs, we examined cross presentation of antigen delivered to less proteolytic early endosomes.

We recently showed that antigen delivery through CD40 targets antigens to early endosomes in BDCA1$^+$ DCs (Chatterjee et al., 2012). We confirmed that anti-CD40 antibody traffics to early endosomes in BDCA3$^+$ DCs after 3 h of continuous uptake, although most of the antibody was found at the cell surface, as for BDCA1$^+$ DCs (Fig. 5 A). Antibody detected intracellularly in both cell types was excluded from Lamp1-positive late endosomes and lysosomes and, instead, overlapped with the endogenous early endosomal marker EEA1. In addition, anti-CD40 antibody accumulated (surface bound and internalized) to similar extents in BDCA3$^+$ DCs and BDCA1$^+$ DCs (Fig. 5 B).

When using anti–CD40-Flu-M1 conjugates in our antigen presentation assay, we found that both BDCA3$^+$ DCs and BDCA1$^+$ DCs were able to cross present early endosomally targeted antigen with comparable efficiencies (Fig. 5 C) and better than when antigen was delivered through DEC205 (see Fig. 7, B and C). Similarly, CD40 targeting of CMV-pp65 peptide also resulted in similar cross presentation by both blood DC subsets, whether unstimulated or TLR7/8 L stimulated (Fig. 5 D). The enhanced cross presentation observed using the anti-CD40 antibody did not result from DC maturation induced by CD40 triggering because targeting anti-CD40 antibody to DCs did not increase their surface maturation markers, nor did it induce the production of inflammatory cytokines (Chatterjee et al., 2012; and unpublished data). Nor did unconjugated anti-CD40 enhance the presentation of Flu-M1 antigen delivered via DEC205 (Chatterjee et al., 2012). In addition, similar results were obtained using an antibody to a second surface receptor, CD11c, whose ligation is not associated with DC maturation but whose internalization also results in delivery to EEA1-positive early endosomes (Fig. 6 A). CD11c-targeted Flu-M1 was cross presented comparably by both BDCA1$^+$ DCs and BDCA3$^+$ DCs (Fig. 6 B).

These results were in sharp contrast with those obtained with late endosomal/lysosomal-targeted anti-DEC205 antibody (Fig. 3 A; and Fig. 7, B and C). This was not a result of differential antibody accumulation because antibodies against DEC205 and CD40 were accumulated by BDCA1$^+$ DCs and BDCA3$^+$ DCs to similar extents (Fig. 7 A). In addition, even pDCs were able to stimulate Flu-M1–specific CD8$^+$ T cells when antigen was delivered via CD40 but not DEC205 (Fig. 7, B and C), implying that even a cell type not normally associated with efficient cross presentation can be induced to do so if the antigen was delivered to early endocytic compartments.

Finally, we compared the ability of BDCA1$^+$ DCs, BDCA3$^+$ DCs, and pDCs to present antigen on MHCII to CD4$^+$ T cells.

Downloaded from http://rupress.org/jem/article-pdf/210/5/1049/1748340/jem_20121251.pdf by guest on 09 February 2026

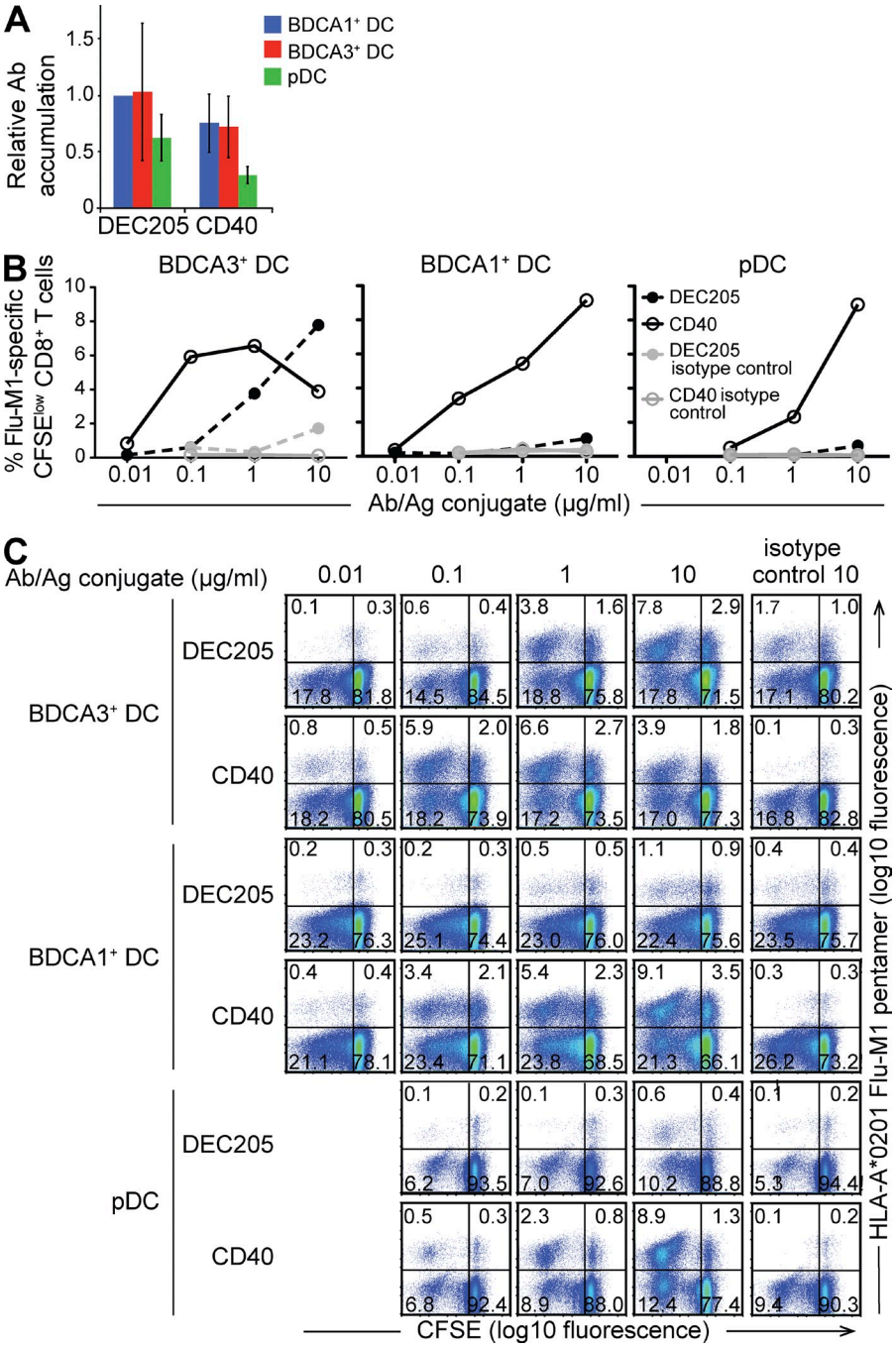

Figure 7. Antigen delivered to early endosomes via CD40 is more efficiently cross presented by all DC subsets than antigen delivered to lysosomes via DEC205. (A) Antibody accumulation. Day 1 DCs were fed with Alexa Fluor 488–labeled anti-DEC205 or anti-CD40 antibody continuously for 3–4 h at 4°C or 37°C. Results were analyzed by flow cytometry. The 4°C MFI was subtracted from the 37°C MFI, and resultant MFI was normalized to BDCA1$^+$ DCs fed with anti-DEC205. MFI was also normalized for the number of fluorophores per antibody. Data shown are the mean MFI ± SD (n = 5 independent experiments). (B and C) Antigen cross presentation via CD40 and DEC205 in DC subsets. Day 1 isolated DCs from HLA-A*0201 donors were fed with anti-DEC205, anti-CD40, or control isotype antibodies conjugated to Flu-M1 (aa 55–72) at indicated doses for 4 h at 37°C. The cells were then washed and cultured with autologous CFSE-labeled CD8$^+$ T cells in the presence of IL-2 and TLR7/8 L. 8–10 d later, Flu-M1–specific CD8$^+$ T cells were detected by staining with Flu-M1 (aa 58–66) pentamer. T cell proliferation was measured by CFSE dilution. The graphs shown in B show frequency of CFSE^{low}, Flu-M1 (aa 58–66) pentamer-positive CD8$^+$ T cells. In C, FACS plots of CD8$^+$ T cells showing CFSE dilution in response to antigen presentation and numbers indicate frequency of CD8$^+$ T cells in each quadrant. Shown is one representative experiment of three.

For these experiments, a NY-ESO-1 peptide was coupled to anti-CD40 or anti-DEC205 antibodies, and antigen presentation was monitored using a NY-ESO-1–specific human CD4$^+$ T cell line. Especially when anti-CD40 was the delivery vehicle, little if any difference was observed in antigen presentation efficiency between the three DC subsets (Fig. 8, left). Presentation after internalization via DEC205 was generally less efficient, as previously observed for mo-DCs (Chatterjee et al., 2012); similarly, there was not a clear difference in efficiency between BDCA1$^+$ DCs and BDCA3$^+$ DCs (Fig. 8, right). Thus, the intracellular destination of internalized antigen appears to be a more important determinant of presentation efficiency than the population of DC being targeted for presentation to both CD4$^+$ and CD8$^+$ T cells.

DISCUSSION

In the mouse, there is excellent evidence to suggest that the CD8α$^+$ DC subset, especially in the spleen, plays a key role in antigen cross presentation in vivo (Dudziak et al., 2007; Hildner et al., 2008). In vitro, several cell biological specializations have been identified that would appear to at least partly explain this function, including careful regulation of

Downloaded from http://rupress.org/jem/article-pdf/210/5/1049/1748340/jem_20121251.pdf by guest on 09 February 2026

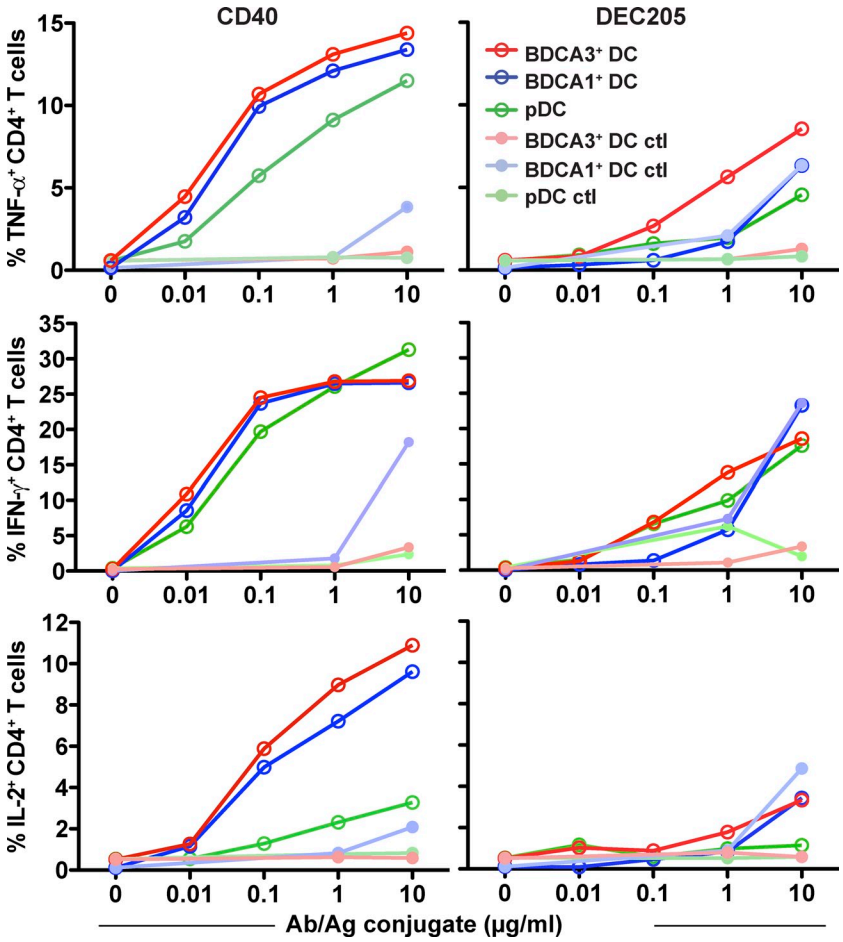

Figure 8. Antigen delivered to early endosomes is presented on MHCII equally by all DC subsets and is more efficiently presented than antigen delivered to lysosomes. Day 1 isolated DCs from HLA-DPB1*0401 donors were fed with anti-DEC205, anti-CD40, or control isotype antibodies conjugated to NY-ESO-1 (aa 154–180) for 1.5 h. Cells were then washed and cultured with an NY-ESO-1–specific CD4+ T cell clone at a ratio of DCs to T cells of 1/1. CD4+ T cells were then stained for intracellular cytokines. The percentage of CD4+ T cells positive for IFN-γ, IL-2, and TNF are depicted. Shown is one representative experiment of four.

lysosomal pH, inactivation of lysosomal proteases by ROS, and the delivery of ER-derived components (Amigorena and Savina, 2010; Segura and Villadangos, 2011). The recent discovery that the human BDCA3+ DC subset shared many surface markers and transcription factors with the murine CD8α+ DC subset suggested that the BDCA3+ DCs were their functional paralog (Robbins et al., 2008). Although in vivo evidence for this possibility is lacking, in vitro evidence for enhanced cross presentation by BDCA3+ DCs relative to other DCs was consistent with this possibility (Bachem et al., 2010; Crozat et al., 2010a; Jongbloed et al., 2010; Poulin et al., 2010). However, the scarcity of these cells made quantitative comparative analysis difficult, and studies thus far relied on the uptake of apoptotic cells or unspecified amounts of viral antigens. Further complicating matters were recent results suggesting that even among mouse DCs, the differences in cross presentation between CD8α+ DCs and other subsets tend to diminish when one controls for the amounts and pathways of antigen uptake (Kamphorst et al., 2010). We reexamined this issue using an improved method for BDCA3+ DC isolation, combined with approaches to antigen loading that allowed for the careful quantitative monitoring of antigen uptake and intracellular fate. We found that with respect to overall antigen presentation capacity, BDCA3+ DCs were fundamentally similar to BDCA1+ DCs. Although BDCA3+ DCs were superior in the cross presentation of antigens delivered by receptors targeted to late endosomes and lysosomes, antigens targeted to early compartments were not cross presented more efficiently. Thus, it seems unlikely that BDCA3+ DCs possess a generalized specialization for cross presentation that greatly distinguish them, at least in vitro, from other DCs unless that mechanism is selectively present only in the lysosomes of BDCA3+ DCs.

The molecular basis for the functional adaptation of BDCA3+ DC lysosomes that enables more efficient cross presentation is unknown. BDCA3+ DCs express lower levels of lysosomal proteases than BDCA1+ DCs, suggesting that perhaps enhanced antigen release into the cytosol is favored by reduced lysosomal degradation. Thus far, we have not demonstrated enhanced NOX-2 activity that might further diminish lysosomal function in BDCA3+ DCs, as occurs in CD8α+ DCs (Savina et al., 2006; Savina et al., 2009; Rybicka et al., 2012). Interestingly, mo-DCs, which exhibit levels of lysosomal proteases similar to monocytes and macrophages (Burster et al., 2005; McCurley and Mellman, 2010), are even poorer than BDCA1+ DCs at cross presentation (Chatterjee et al., 2012).

Downloaded from http://rupress.org/jem/article-pdf/210/5/1049/1748340/jem_20121251.pdf by guest on 09 February 2026

Alternatively, BDCA3$^+$ DCs may have developed specialized machinery to transfer antigen to the cytosol. The ER protein retrotranslocation machinery normally involved in the degradation of misfolded ER proteins has been proposed to have a role in the transport of antigen from endocytic compartments to the cytosol. However, the molecular composition of the ER-translocation machinery remains somewhat elusive. Recently, Sec22b has been shown to control the recruitment of ER-resident proteins to the phagosome and increases cross presentation from phago-lysosomes in CD8α^+ DCs, possibly by favoring antigen egress to the cytosol (Cebrian et al., 2011). The lysosomes of CD8α^+ DCs have also been reported to be more "leaky" to internalized cytochrome *C* (Lin et al., 2008). Although this may reflect the recruitment of an ER-translocation mechanism, it may simply be that BDCA3$^+$ DC lysosomes are more susceptible to transient physical rupture, which would also result in delivery of antigens to the cytosol. Indeed, release of internalized antigen in the cytosol by osmotic disruption of the endosomes leads to antigen cross presentation even in nonprofessional antigen-presenting cells (Moore et al., 1988). Although more work will be required to define the mechanism of antigen escape from endocytic compartments, our results demonstrate that this step is rate limiting to antigen access to the MHCI pathway. When this barrier was effectively removed by using fusion-competent IAV or KBMA *L. monocytogenes* to deliver viral antigen to the cytosol from late endosomes or lysosomes, the difference in cross presentation efficiency between BDCA3$^+$ DCs and BDCA1$^+$ DCs disappeared.

We recently demonstrated that targeting antigens to early endosomes, as compared with late endosomes and lysosomes, results in more efficient cross presentation in both BDCA1$^+$ DCs and mo-DCs (Chatterjee et al., 2012). BDCA3$^+$ DCs also cross present antigens delivered to early endosomes 10–100-fold more efficiently than antigens delivered to lysosomes, even though less antigen was internalized by coupling to anti-CD40 (Fig. 7). This result suggests that even though BDCA3$^+$ DC lysosomes may be adapted for cross presentation (or at least more so than BDCA1$^+$ DC lysosomes), they are not optimized for this process. Importantly, we show that the three human blood DC subsets tested can cross present antigen targeted to early endosomes, with BDCA1$^+$ DCs and BDCA3$^+$ DCs possessing similar capacities for antigen cross presentation to CD8$^+$ T cells in an in vitro recall assay. Although the situation may be different for resident tissue DCs in humans, these results imply an overall similarity in the cell biological mechanisms underlying the events essential to antigen cross presentation across all DC subsets.

Another observation that is worth mentioning is the inability of anti-DEC205 antibody to enable the cross presentation of antigen by BDCA1$^+$ DCs. This is in contrast to other studies of both mouse and human DCs (Hawiger et al., 2001; Bozzacco et al., 2007; Idoyaga et al., 2011). In our experiments, we coupled extended peptides to anti-DEC205 antibody (Chatterjee et al., 2012), whereas most previous work has relied on direct fusions or conjugations of peptides or intact proteins (typically ovalbumin in the mouse). Because we have used the same anti–human DEC205 antibody as in previous studies (Tsuji et al., 2011), we suspect that our chemically coupled peptides are more sensitive to degradation and, therefore, to illuminating the efficiency differences between BDCA3$^+$ DCs and BDCA1$^+$ DCs. Certainly uptake efficiency and intracellular targeting were not different between the two cell types. Peptides were chosen because this approach is easily scalable and permits the type of quality control that may help the transition of this platform to late stage clinical development and application in patients. The anti–DEC205-peptide conjugates also appeared to reveal the only demonstrable difference in cross presentation efficiency between the DC subsets studied.

Our findings have further implications for the design of potential DC-targeted vaccines. BDCA3$^+$ DCs are a rare subset of DCs in the blood, where they represent <5% of the total blood DCs. Targeting antigens to early endosomes not only increases cross presentation by BDCA3$^+$ DCs but also extends cross presentation to more abundant DC subsets and thus could potentially maximize CD8$^+$ T cell responses in vivo. Thus, selective targeting of antigens to BDCA3$^+$ DCs via specifically expressed receptors such as DNGR1 (Schreibelt et al., 2012) may not offer an inherent advantage. In vivo studies will be needed to determine the relative contribution of the human DC subsets to the induction of CD8$^+$ T cell immunity.

DC function may be affected by cytokines in the environment. GM-CSF has recently been shown to enhance the cross presentation capacity of mouse CD8α^+ DCs (Sathe et al., 2011; Zhan et al., 2012). In our study, the capacity of BDCA1$^+$ DCs and BDCA3$^+$ DCs to cross present antigens was evaluated after overnight culture in the presence of GM-CSF. Because GM-CSF was critical to DC survival in vitro (unpublished data), we were unable to assess whether GM-CSF also affected human blood DC function.

Factors other than the capacity for cross presentation may also be important for DC function in vivo. In the skin, resident BDCA3$^+$ DCs constitutively produce IL-10, possibly in a vitamin D3–dependent manner, and thus mediate T cell tolerance rather than immunity at steady state (Chu et al., 2012). In the mouse, stimulation of TLRs and the ligation of CD40 induce CD8α^+ DCs not only to cross present effectively but also to express CD70, a costimulatory molecule which favors the priming of CD8$^+$ T cell responses and the generation of CD8$^+$ T cell memory (Hendriks et al., 2000; Soares et al., 2007). Whether BDCA3$^+$ DCs also share this characteristic will be important to examine to better understand the role of BDCA3$^+$ DCs in vivo.

MATERIALS AND METHODS

Reagents. Anti-DEC205 antibody (3G9) is from Celldex Therapeutics Inc., whereas anti-CD40 antibody (S2C6) is from Seattle Genetics and American Type Culture Collection. Antibodies against CD11c (Bly6), CD3 (SK7), CD4 (Leu-3a/SK3), CD8 (SK1), CD8 (RPA-T8), CD14 (MΦP9), CD19 (Leu-12), CD40 (5C3), CD83 (HB15e), CD86 (FUN-1), HLA-DR (TÜ36 and L243), and Lamp1 (H4A3) are from BD; antibodies against

Downloaded from http://rupress.org/jem/article-pdf/210/5/1049/1748340/jem_20121251.pdf by guest on 09 February 2026

BDCA1 (AD5-8E7), BDCA3 (AD5-14H12), and BDCA4 (AD5-17F6) are from Miltenyi Biotec; and antibodies against HLA-ABC (W6/32) are from BioLegend or eBioscience. Anti-EEA1 is from Cell Signaling Technology. Anti–Cathepsin D and Cathepsin S are from EMD Millipore, anti-actin and –Cathepsin B (CB59-4B11) are from Sigma-Aldrich, and mouse anti–Cathepsin L (33/1) is from Santa Cruz Biotechnology, Inc. Secondary reagents (anti-FITC Alexa Fluor 488, Streptavidin Alexa Fluor 555, anti–rabbit Alexa Fluor 546, Streptavidin Alexa Fluor 647, and anti–human IgG Alexa Fluor 647) are from Invitrogen/Molecular Probes. The anti-Influenza HA antibody, PINDA, was a gift from A. Helenius (ETH Zürich, Switzerland). Anti-DEC205, -CD40, and -CD11c antibodies were conjugated to extended peptides Flu-M1 (aa 55–72), CMV-pp65 (aa 488–508), and NY-ESO-1 (aa 154–180) as described elsewhere (Chatterjee et al., 2012). Antibodies had approximately the same number of peptides per molecule by mass spectrometry and remained >95% monomeric (unpublished data). HLA-A*0201 peptides (Flu-M1 [aa 58–66], CMV-pp65 [aa 495–503], and HIV-p17 [aa 77–85] as a negative control) are from Anaspec, whereas NY-ESO-1 (aa 157–170) is from Elim. Flu-M1 (aa 58–66) and CMV-pp65 (aa 495–503) pentamers are from Proimmune.

Cell isolation and culture. This study was approved by the Genentech Institutional Review Board. As previously described (Smed-Sörensen et al., 2005), healthy blood donors underwent automated leukapheresis, and enriched populations of lymphocytes and monocytes were obtained by counterflow centrifugal elutriation. BDCA1$^+$ DCs, BDCA3$^+$ DCs, and pDCs were isolated from the monocyte/DC fraction using magnetic bead isolation reagents and AutoMACS technology (Miltenyi Biotec). The CD1c/BDCA1$^+$ DC isolation kit was used for isolation of BDCA1$^+$ DCs from one third of the monocyte/DC fraction. pDCs and BDCA3$^+$ DCs were sequentially isolated from two thirds of the monocyte/DC fraction. pDCs were isolated using anti–BDCA4-biotin antibody (Miltenyi Biotec) followed by anti-biotin microbeads (100 µl/10^6 cells, each). Before BDCA3 isolation, CD123$^+$ cells and pDCs were depleted from the fraction using CD123 microbeads and BDCA4 microbeads. BDCA3$^+$ DCs were enriched using anti–BDCA3-biotin (55 µl total) antibody and anti-biotin beads (15 µl total). After isolation and before performing experiments, DCs were rested overnight in 5 ml polypropylene, round-bottom tubes (Falcon) at 10^6 cells/ml in complete medium (RPMI 1640 + GlutaMAX supplemented with 10% FCS, 100 U/ml penicillin + 100 µg/ml streptomycin, and 10 mM Hepes), and 2 ng/ml GM-CSF (PeproTech) for BDCA1$^+$ DCs and BDCA3$^+$ DCs, and 10 ng/ml IL-3 (R&D Systems) for pDCs. In some experiments, DCs were exposed to 1 µg/ml TLR7/8 agonist (CL075; InvivoGen) overnight to induce DC maturation. CD8$^+$ T cells were isolated from HLA-A*0201 elutriated lymphocyte fraction using the CD8$^+$ T cell isolation kit, followed by separation on MACS LS columns (Miltenyi Biotec), and overnight culture at 10×10^6 cells/ml in complete medium for use the following day. Mo-DCs were derived in 5–7 d from CD14$^+$ monocytes cultured in R10 supplemented with 100 ng/ml GM-CSF (PeproTech) and 6.5 ng/ml IL-4 (R&D Systems). The percentage of live cells after overnight culture was determined by flow cytometry by gating out dead cells based on forward scatter and side scatter. DCs were only used if viability was >65%. DCs were not used if one subset was significantly more viable than another.

DC surface maturation markers and cytokine secretion. PBMCs were surface stained with antibodies against CD14, CD19, CD11c, BDCA1 or BDCA3, DEC205, CD83, CD86, CD40, HLA-ABC, and HLA-DR or corresponding isotype controls. Cells were washed, fixed in 1% paraformaldehyde (PFA), and acquired using a FACS Canto II (BD). Fluorescence signal was analyzed using FlowJo software and normalized to exclude fluorescence from nonspecific isotype control binding. After overnight culture in the presence or absence of 1 µg/ml TLR7/8 L, isolated DCs were harvested, washed, and surface stained with antibodies against BDCA1 or BDCA3, CD14, DEC205, CD83, CD86, CD40, HLA-ABC, and HLA-DR or corresponding isotype controls. DCs were washed, fixed in 1% PFA, and acquired using a FACS Canto II. Fluorescence signal was analyzed using FlowJo software and normalized to exclude fluorescence from nonspecific isotype control binding. Supernatants were harvested and cytokines were measured by Luminex (Bio-Rad Laboratories) or ELISA (IFN-α; PBL Interferon Source).

Ovalbumin accumulation experiments. Cells were continuously incubated with 5 µg/ml ovalbumin-A488 (Invitrogen) for 20 min at either 4 or 37°C. Cells were then washed and stained for CD14 and BDCA1 or BDCA3, fixed in PFA, and analyzed by flow cytometry.

Antibody targeted antigen cross presentation assay. HLA-A*0201 DCs were incubated for 4–6 h in the presence of 0.1–10 µg/ml of antibody-peptide conjugates or 2.5–250 ng/ml of preprocessed peptide. After antigen uptake, DCs were washed extensively to remove free antibody or peptide and cultured with 1.5×10^6 CFSE (Invitrogen)-labeled CD8$^+$ T cells at a DC/T cell ratio of 1:30 (unless otherwise indicated), in the presence of 20 U/ml IL-2 (Roche) and 1 µg/ml TLR7/8 L. After 8–10 d, cells were harvested and stained with Flu-M1 (aa 58–66) or CMV-pp65 (aa 495–503) pentamer for 15 min at room temperature, followed by labeling with antibodies against CD3, CD8, CD4, and CD19, fixation, and analysis by flow cytometry. Dead cells were gated out based on forward scatter and side scatter.

MHCII presentation assay. HLA-DPB1*0401 DCs were incubated for 1.5 h in the presence of 0.1–10 µg/ml of antibody-peptide conjugates or 2.5–25 µg/ml of peptide control. After antigen uptake, DCs were washed and cocultured with a NY-ESO-1–specific human CD4$^+$ T cell clone for 7–9 h at DC to T cell ratios of 1:1. 2 h into the co-culture, brefeldin A (eBioscience) was added to prevent cytokine secretion. After co-culture, cells were stained for surface markers, fixed, permeabilized, and labeled for intracellular IFN-γ, IL-2, and TNF. Cells were analyzed by flow cytometry.

Antibody accumulation experiments. Cells were incubated with 5 µg/ml anti-CD40 or anti-DEC205 antibodies conjugated to Alexa Fluor 488 (mAb labeling kit; Invitrogen) at 4 or 37°C for 4–6 h. Cells were then stained for CD14 and BDCA1 or BDCA3, fixed in PFA, and analyzed by flow cytometry.

Antibody internalization experiment. Cells were incubated with 5 µg/ml anti-DEC205 or isotype control antibodies conjugated to Alexa Fluor 488 at 4°C for 30 min. Cells were then washed in cold media and incubated for the indicated times at 37°C. At each time point, cells were transferred to 4°C and labeled with an Alexa Fluor 647–labeled anti–human IgG antibody at a dilution 1:2,000. Cells were then fixed in PFA and analyzed by flow cytometry.

Immunofluorescence. After accumulation of 5 µg/ml A488-conjugated anti-CD40, anti-DEC205, or anti-CD11c antibodies at 37°C for 4–6 h, BDCA1$^+$ DCs or BDCA3$^+$ DCs were washed in serum-free medium and spotted at 50,000-100,000 cells on Alcian blue–coated glass coverslips for 10–15 min at room temperature. Upon adherence, cells were fixed in 4% PFA (Electron Microscopy Source) for 15 min, followed by washes in PBS. Cells were permeabilized in 0.05% saponin (Sigma-Aldrich) and counterstained as indicated. When biotinylated antibodies were used, endogenous biotin was blocked using an excess of unlabeled streptavidin and biotin (endogenous biotin blocking kit; Invitrogen), followed by labeling with biotinylated antibodies. After primary and secondary antibody labeling, cells were washed in PBS and water, and then mounted onto glass slides using Prolong Gold with DAPI (Invitrogen/Molecular Probes). Imaging was performed on a confocal microscope (SP5; Leica), using a 100× oil objective (NA: 1.47), zoom 5, and data acquired using LAS imaging software (Leica).

Protease levels in DC subsets. Cells were lysed at 4°C in a buffer containing 1% (vol/vol) Triton X-100, 0.1% (wt/vol) SDS, 20 mM Tris, pH 7.4, and protease inhibitors (Complete mini; Roche). The cell lysate was adjusted for equal total protein, separated by SDS-PAGE, and transferred to a PVDF membrane (Invitrogen) using standard protocols. Immunoblotting

Downloaded from http://rupress.org/jem/article-pdf/210/5/1049/1748340/jem_20121251.pdf by guest on 09 February 2026

was performed with the indicated antibodies. All secondary antibodies used for Western blotting were conjugated to HRP (Jackson ImmunoResearch Laboratories). Membranes were developed using the ECL system (Thermo Fisher Scientific).

Transfection. Immediately after isolation, BDCA1$^+$ DCs and BDCA3$^+$ DCs were transiently transfected with a plasmid encoding Flu-M1 (aa 55–72)-EGFP fusion protein using the Human Dendritic Cell Nucleofactor kit (Amaxa). In brief, 2×10^6 DCs were resuspended in transfection buffer, mixed with 1 µg plasmid and electroporated using program U-002 on a Nucleofector 2b device (Lonza). Immediately after transfection, cells were mixed with warm complete medium containing GM-CSF and cultured at 10^6 cells/ml in the presence or absence of TLR7/8 L. EGFP expression was assayed by flow cytometry 16 h later.

Replication incompetent IAV antigen presentation assay. Replication incompetent viruses were obtained as described elsewhere (Smed-Sörensen et al., 2012). Replication incompetent virus was made fusion incompetent after treatment with a low pH buffer (Stegmann et al., 1987). In brief, IAV was incubated for 5 min at 37°C in pH 4.5 buffer (or pH 7.4 as control), containing 135 mM NaCl, 15 mM Sodium Citrate, 10 mM MES, and 5 mM Hepes. DCs from HLA-A*0201 donors were infected with 600,000 infectious particles (as assessed in an MDCK plaque assay) of IAV per 1,000,000 DCs (0.6 MOI) for 6 h and washed before coculturing with CFSE-labeled autologous CD8$^+$ T cells at indicated ratios. After 8–10 d, cells were harvested and stained with Flu-M1 (aa 58–66) pentamer for 15 min at room temperature, followed by labeling with antibodies against CD3, CD8, CD4, and CD19, fixation, and analysis by flow cytometry.

Flu-M1–expressing *L. monocytogenes* antigen presentation assay. Phagosomal escape competent (Δ*actA* Δ*inlB* Δ*uvrAB* strain: BH3446) or incompetent (Δ*hly* Δ*uvrAB* strain: BH3448) KBMA *L. monocytogenes* that express Flu-M1 + ovalbumin fusion peptides [ActAN100-Flu-M1 (aa 58–66) − OVA (aa 257–264)] or corresponding non–Flu-M1–expressing strains (Lm583 for BH3446 and Lm918 for BH3448) were obtained from Aduro Biotech, Inc. and have been described in part previously (Skoberne et al., 2008). Bacteria were incubated with HLA-A*0201 BDCA1$^+$ DCs and BDCA3$^+$ DCs for 1 h in medium without antibiotics. After incubation, DCs were washed extensively to remove excess bacteria and cocultured with autologous CFSE-labeled CD8$^+$ T cells + 20 U/ml IL-2 at a DC/T cell ratio of 1:30 for 8–10 d in the presence of antibiotics (100 U/ml penicillin, 100 µg/ml streptomycin, and 20 µg/ml gentamicin) to kill extracellular bacteria. After co-culture, cells were harvested and stained with Flu-M1 (aa 58–66) pentamer for 15 min at room temperature, followed by labeling with antibodies against CD3, CD8, CD4, and CD19, fixation, and analysis by flow cytometry.

The authors would like to thank the Genentech Research Blood Donation Program and the Blood Centers of the Pacific, especially Yelena Dayter for her elutriation expertise. We thank members of the Mellman laboratory for discussions and advice. Finally, we remember Ralph Steinman fondly, and thank him for his thoughtful comments on this project.

C. Chalouni, B.-C. Lee, R. Vandlen, I. Mellman, and L. Delamarre are employees of Genentech, T. Keler is an employee of Celldex Therapeutics Inc., and P. Lauer and D. Brockstedt are employees of Aduro BioTech Inc; they hence declare a competing financial interest.

Submitted: 11 June 2012
Accepted: 15 March 2013

REFERENCES

Accapezzato, D., V. Visco, V. Francavilla, C. Molette, T. Donato, M. Paroli, M.U. Mondelli, M. Doria, M.R. Torrisi, and V. Barnaba. 2005. Chloroquine enhances human CD8$^+$ T cell responses against soluble antigens in vivo. *J. Exp. Med.* 202:817–828. http://dx.doi.org/10.1084/jem.20051106

Amigorena, S., and A. Savina. 2010. Intracellular mechanisms of antigen cross presentation in dendritic cells. *Curr. Opin. Immunol.* 22:109–117. http://dx.doi.org/10.1016/j.coi.2010.01.022

Bachem, A., S. Güttler, E. Hartung, F. Ebstein, M. Schaefer, A. Tannert, A. Salama, K. Movassaghi, C. Opitz, H.W. Mages, et al. 2010. Superior antigen cross-presentation and XCR1 expression define human CD11c$^+$CD141$^+$ cells as homologues of mouse CD8$^+$ dendritic cells. *J. Exp. Med.* 207:1273–1281. http://dx.doi.org/10.1084/jem.20100348

Banchereau, J., and R.M. Steinman. 1998. Dendritic cells and the control of immunity. *Nature.* 392:245–252. http://dx.doi.org/10.1038/32588

Belizaire, R., and E.R. Unanue. 2009. Targeting proteins to distinct subcellular compartments reveals unique requirements for MHC class I and II presentation. *Proc. Natl. Acad. Sci. USA.* 106:17463–17468. http://dx.doi.org/10.1073/pnas.0908583106

Bozzacco, L., C. Trumpfheller, F.P. Siegal, S. Mehandru, M. Markowitz, M. Carrington, M.C. Nussenzweig, A.G. Piperno, and R.M. Steinman. 2007. DEC-205 receptor on dendritic cells mediates presentation of HIV gag protein to CD8+ T cells in a spectrum of human MHC I haplotypes. *Proc. Natl. Acad. Sci. USA.* 104:1289–1294. http://dx.doi.org/10.1073/pnas.0610383104

Burgdorf, S., A. Kautz, V. Böhnert, P.A. Knolle, and C. Kurts. 2007. Distinct pathways of antigen uptake and intracellular routing in CD4 and CD8 T cell activation. *Science.* 316:612–616. http://dx.doi.org/10.1126/science.1137971

Burster, T., A. Beck, E. Tolosa, P. Schnorrer, R. Weissert, M. Reich, M. Kraus, H. Kalbacher, H.U. Häring, E. Weber, et al. 2005. Differential processing of autoantigens in lysosomes from human monocyte-derived and peripheral blood dendritic cells. *J. Immunol.* 175:5940–5949.

Cebrian, I., G. Visentin, N. Blanchard, M. Jouve, A. Bobard, C. Moita, J. Enninga, L.F. Moita, S. Amigorena, and A. Savina. 2011. Sec22b regulates phagosomal maturation and antigen crosspresentation by dendritic cells. *Cell.* 147:1355–1368. http://dx.doi.org/10.1016/j.cell.2011.11.021

Cervantes-Barragan, L., K.L. Lewis, S. Firner, V. Thiel, S. Hugues, W. Reith, B. Ludewig, and B. Reizis. 2012. Plasmacytoid dendritic cells control T-cell response to chronic viral infection. *Proc. Natl. Acad. Sci. USA.* 109:3012–3017. http://dx.doi.org/10.1073/pnas.1117359109

Chatterjee, B., A. Smed-Sörensen, L. Cohn, C. Chalouni, R. Vandlen, B.C. Lee, J. Widger, T. Keler, L. Delamarre, and I. Mellman. 2012. Internalization and endosomal degradation of receptor-bound antigens regulate the efficiency of cross presentation by human dendritic cells. *Blood.* 120:2011–2020. http://dx.doi.org/10.1182/blood-2012-01-402370

Chu, C.C., N. Ali, P. Karagiannis, P. Di Meglio, A. Skowera, L. Napolitano, G. Barinaga, K. Grys, E. Sharif-Paghaleh, S.N. Karagiannis, et al. 2012. Resident CD141 (BDCA3)$^+$ dendritic cells in human skin produce IL-10 and induce regulatory T cells that suppress skin inflammation. *J. Exp. Med.* 209:935–945. http://dx.doi.org/10.1084/jem.20112583

Crozat, K., R. Guiton, V. Contreras, V. Feuillet, C.A. Dutertre, E. Ventre, T.P. Vu Manh, T. Baranek, A.K. Storset, J. Marvel, et al. 2010a. The XC chemokine receptor 1 is a conserved selective marker of mammalian cells homologous to mouse CD8α$^+$ dendritic cells. *J. Exp. Med.* 207:1283–1292. http://dx.doi.org/10.1084/jem.20100223

Crozat, K., R. Guiton, M. Guilliams, S. Henri, T. Baranek, I. Schwartz-Cornil, B. Malissen, and M. Dalod. 2010b. Comparative genomics as a tool to reveal functional equivalences between human and mouse dendritic cell subsets. *Immunol. Rev.* 234:177–198. http://dx.doi.org/10.1111/j.0105-2896.2009.00868.x

Dudziak, D., A.O. Kamphorst, G.F. Heidkamp, V.R. Buchholz, C. Trumpfheller, S. Yamazaki, C. Cheong, K. Liu, H.W. Lee, C.G. Park, et al. 2007. Differential antigen processing by dendritic cell subsets in vivo. *Science.* 315:107–111. http://dx.doi.org/10.1126/science.1136080

Dzionek, A., A. Fuchs, P. Schmidt, S. Cremer, M. Zysk, S. Miltenyi, D.W. Buck, and J. Schmitz. 2000. BDCA-2, BDCA-3, and BDCA-4: three markers for distinct subsets of dendritic cells in human peripheral blood. *J. Immunol.* 165:6037–6046.

Garrett, W.S., L.M. Chen, R. Kroschewski, M. Ebersold, S. Turley, S. Trombetta, J.E. Galán, and I. Mellman. 2000. Developmental control of endocytosis in dendritic cells by Cdc42. *Cell.* 102:325–334. http://dx.doi.org/10.1016/S0092-8674(00)00038-6

Hawiger, D., K. Inaba, Y. Dorsett, M. Guo, K. Mahnke, M. Rivera, J.V. Ravetch, R.M. Steinman, and M.C. Nussenzweig. 2001. Dendritic cells induce

Downloaded from http://rupress.org/jem/article-pdf/210/5/1049/1748340/jem_20121251.pdf by guest on 09 February 2026

peripheral T cell unresponsiveness under steady state conditions in vivo. *J. Exp. Med.* 194:769–779. http://dx.doi.org/10.1084/jem.194.6.769

Heath, W.R., and F.R. Carbone. 2009. Dendritic cell subsets in primary and secondary T cell responses at body surfaces. *Nat. Immunol.* 10:1237–1244. http://dx.doi.org/10.1038/ni.1822

Hendriks, J., L.A. Gravestein, K. Tesselaar, R.A. van Lier, T.N. Schumacher, and J. Borst. 2000. CD27 is required for generation and long-term maintenance of T cell immunity. *Nat. Immunol.* 1:433–440. http://dx.doi.org/10.1038/80877

Hildner, K., B.T. Edelson, W.E. Purtha, M. Diamond, H. Matsushita, M. Kohyama, B. Calderon, B.U. Schraml, E.R. Unanue, M.S. Diamond, et al. 2008. Batf3 deficiency reveals a critical role for CD8alpha+ dendritic cells in cytotoxic T cell immunity. *Science.* 322:1097–1100. http://dx.doi.org/10.1126/science.1164206

Hornung, V., J. Schlender, M. Guenthner-Biller, S. Rothenfusser, S. Endres, K.K. Conzelmann, and G. Hartmann. 2004. Replication-dependent potent IFN-alpha induction in human plasmacytoid dendritic cells by a single-stranded RNA virus. *J. Immunol.* 173:5935–5943.

Idoyaga, J., A. Lubkin, C. Fiorese, M.H. Lahoud, I. Caminschi, Y. Huang, A. Rodriguez, B.E. Clausen, C.G. Park, C. Trumpfheller, and R.M. Steinman. 2011. Comparable T helper 1 (Th1) and CD8 T-cell immunity by targeting HIV gag p24 to CD8 dendritic cells within antibodies to Langerin, DEC205, and Clec9A. *Proc. Natl. Acad. Sci. USA.* 108:2384–2389. http://dx.doi.org/10.1073/pnas.1019547108

Jiang, A., O. Bloom, S. Ono, W. Cui, J. Unternaehrer, S. Jiang, J.A. Whitney, J. Connolly, J. Banchereau, and I. Mellman. 2007. Disruption of E-cadherin-mediated adhesion induces a functionally distinct pathway of dendritic cell maturation. *Immunity.* 27:610–624. http://dx.doi.org/10.1016/j.immuni.2007.08.015

Joffre, O., M.A. Nolte, R. Spörri, and C. Reis e Sousa. 2009. Inflammatory signals in dendritic cell activation and the induction of adaptive immunity. *Immunol. Rev.* 227:234–247. http://dx.doi.org/10.1111/j.1600-065X.2008.00718.x

Jongbloed, S.L., A.J. Kassianos, K.J. McDonald, G.J. Clark, X. Ju, C.E. Angel, C.J. Chen, P.R. Dunbar, R.B. Wadley, V. Jeet, et al. 2010. Human CD141$^+$ (BDCA-3)$^+$ dendritic cells (DCs) represent a unique myeloid DC subset that cross-presents necrotic cell antigens. *J. Exp. Med.* 207:1247–1260. http://dx.doi.org/10.1084/jem.20092140

Kamphorst, A.O., P. Guermonprez, D. Dudziak, and M.C. Nussenzweig. 2010. Route of antigen uptake differentially impacts presentation by dendritic cells and activated monocytes. *J. Immunol.* 185:3426–3435. http://dx.doi.org/10.4049/jimmunol.1001205

Kumagai, Y., H. Kumar, S. Koyama, T. Kawai, O. Takeuchi, and S. Akira. 2009. Cutting edge: TLR-dependent viral recognition along with type I IFN positive feedback signaling masks the requirement of viral replication for IFN-alpha production in plasmacytoid dendritic cells. *J. Immunol.* 182:3960–3964. http://dx.doi.org/10.4049/jimmunol.0804315

Lanzavecchia, A., and F. Sallusto. 2001. Regulation of T cell immunity by dendritic cells. *Cell.* 106:263–266. http://dx.doi.org/10.1016/S0092-8674(01)00455-X

Lin, M.L., Y. Zhan, A.I. Proietto, S. Prato, L. Wu, W.R. Heath, J.A. Villadangos, and A.M. Lew. 2008. Selective suicide of cross-presenting CD8+ dendritic cells by cytochrome c injection shows functional heterogeneity within this subset. *Proc. Natl. Acad. Sci. USA.* 105:3029–3034. http://dx.doi.org/10.1073/pnas.0712394105

Mantegazza, A.R., A. Savina, M. Vermeulen, L. Pérez, J. Geffner, O. Hermine, S.D. Rosenzweig, F. Faure, and S. Amigorena. 2008. NADPH oxidase controls phagosomal pH and antigen cross-presentation in human dendritic cells. *Blood.* 112:4712–4722. http://dx.doi.org/10.1182/blood-2008-01-134791

McCurley, N., and I. Mellman. 2010. Monocyte-derived dendritic cells exhibit increased levels of lysosomal proteolysis as compared to other human dendritic cell populations. *PLoS ONE.* 5:e11949. http://dx.doi.org/10.1371/journal.pone.0011949

Mittag, D., A.I. Proietto, T. Loudovaris, S.I. Mannering, D. Vremec, K. Shortman, L. Wu, and L.C. Harrison. 2011. Human dendritic cell subsets from spleen and blood are similar in phenotype and function but modified by donor health status. *J. Immunol.* 186:6207–6217. http://dx.doi.org/10.4049/jimmunol.1002632

Moore, M.W., F.R. Carbone, and M.J. Bevan. 1988. Introduction of soluble protein into the class I pathway of antigen processing and presentation. *Cell.* 54:777–785. http://dx.doi.org/10.1016/S0092-8674(88)91043-4

Peng, Y., and K.B. Elkon. 2011. Autoimmunity in MFG-E8-deficient mice is associated with altered trafficking and enhanced cross-presentation of apoptotic cell antigens. *J. Clin. Invest.* 121:2221–2241. http://dx.doi.org/10.1172/JCI43254

Poulin, L.F., M. Salio, E. Griessinger, F. Anjos-Afonso, L. Craciun, J.L. Chen, A.M. Keller, O. Joffre, S. Zelenay, E. Nye, et al. 2010. Characterization of human DNGR-1$^+$ BDCA3$^+$ leukocytes as putative equivalents of mouse CD8α^+ dendritic cells. *J. Exp. Med.* 207:1261–1271. http://dx.doi.org/10.1084/jem.20092618

Poulin, L.F., Y. Reyal, H. Uronen-Hansson, B.U. Schraml, D. Sancho, K.M. Murphy, U.K. Håkansson, L.F. Moita, W.W. Agace, D. Bonnet, and C. Reis e Sousa. 2012. DNGR-1 is a specific and universal marker of mouse and human Batf3-dependent dendritic cells in lymphoid and nonlymphoid tissues. *Blood.* 119:6052–6062. http://dx.doi.org/10.1182/blood-2012-01-406967

Robbins, S.H., T. Walzer, D. Dembélé, C. Thibault, A. Defays, G. Bessou, H. Xu, E. Vivier, M. Sellars, P. Pierre, et al. 2008. Novel insights into the relationships between dendritic cell subsets in human and mouse revealed by genome-wide expression profiling. *Genome Biol.* 9:R17. http://dx.doi.org/10.1186/gb-2008-9-1-r17

Rybicka, J.M., D.R. Balce, S. Chaudhuri, E.R. Allan, and R.M. Yates. 2012. Phagosomal proteolysis in dendritic cells is modulated by NADPH oxidase in a pH-independent manner. *EMBO J.* 31:932–944. http://dx.doi.org/10.1038/emboj.2011.440

Sathe, P., J. Pooley, D. Vremec, J. Mintern, J.O. Jin, L. Wu, J.Y. Kwak, J.A. Villadangos, and K. Shortman. 2011. The acquisition of antigen cross-presentation function by newly formed dendritic cells. *J. Immunol.* 186:5184–5192. http://dx.doi.org/10.4049/jimmunol.1002683

Savina, A., C. Jancic, S. Hugues, P. Guermonprez, P. Vargas, I.C. Moura, A.M. Lennon-Duménil, M.C. Seabra, G. Raposo, and S. Amigorena. 2006. NOX2 controls phagosomal pH to regulate antigen processing during crosspresentation by dendritic cells. *Cell.* 126:205–218. http://dx.doi.org/10.1016/j.cell.2006.05.035

Savina, A., A. Peres, I. Cebrian, N. Carmo, C. Moita, N. Hacohen, L.F. Moita, and S. Amigorena. 2009. The small GTPase Rac2 controls phagosomal alkalinization and antigen crosspresentation selectively in CD8(+) dendritic cells. *Immunity.* 30:544–555. http://dx.doi.org/10.1016/j.immuni.2009.01.013

Schreibelt, G., L.J. Klinkenberg, L.J. Cruz, P.J. Tacken, J. Tel, M. Kreutz, G.J. Adema, G.D. Brown, C.G. Figdor, and I.J. de Vries. 2012. The C-type lectin receptor CLEC9A mediates antigen uptake and (cross-)presentation by human blood BDCA3+ myeloid dendritic cells. *Blood.* 119:2284–2292. http://dx.doi.org/10.1182/blood-2011-08-373944

Segura, E., and J.A. Villadangos. 2011. A modular and combinatorial view of the antigen cross-presentation pathway in dendritic cells. *Traffic.* 12:1677–1685. http://dx.doi.org/10.1111/j.1600-0854.2011.01254.x

Segura, E., J. Valladeau-Guilemond, M.H. Donnadieu, X. Sastre-Garau, V. Soumelis, and S. Amigorena. 2012. Characterization of resident and migratory dendritic cells in human lymph nodes. *J. Exp. Med.* 209:653–660. http://dx.doi.org/10.1084/jem.20111457

Shortman, K., and W.R. Heath. 2010. The CD8+ dendritic cell subset. *Immunol. Rev.* 234:18–31. http://dx.doi.org/10.1111/j.0105-2896.2009.00870.x

Skoberne, M., A. Yewdall, K.S. Bahjat, E. Godefroy, P. Lauer, E. Lemmens, W. Liu, W. Luckett, M. Leong, T.W. Dubensky, et al. 2008. KBMA Listeria monocytogenes is an effective vector for DC-mediated induction of antitumor immunity. *J. Clin. Invest.* 118:3990–4001. http://dx.doi.org/10.1172/JCI31350

Smed-Sörensen, A., K. Loré, J. Vasudevan, M.K. Louder, J. Andersson, J.R. Mascola, A.L. Spetz, and R.A. Koup. 2005. Differential susceptibility to human immunodeficiency virus type 1 infection of myeloid and plasmacytoid dendritic cells. *J. Virol.* 79:8861–8869. http://dx.doi.org/10.1128/JVI.79.14.8861-8869.2005

Smed-Sörensen, A., C. Chalouni, B. Chatterjee, L. Cohn, P. Blattmann, N. Nakamura, L. Delamarre, and I. Mellman. 2012. Influenza A virus infection of human primary dendritic cells impairs their ability to

Downloaded from http://rupress.org/jem/article-pdf/210/5/1049/1748340/jem_20121251.pdf by guest on 09 February 2026

cross-present antigen to CD8 T cells. *PLoS Pathog.* 8:e1002572. http://dx.doi.org/10.1371/journal.ppat.1002572

Soares, H., H. Waechter, N. Glaichenhaus, E. Mougneau, H. Yagita, O. Mizenina, D. Dudziak, M.C. Nussenzweig, and R.M. Steinman. 2007. A subset of dendritic cells induces $CD4^+$ T cells to produce IFN-γ by an IL-12–independent but CD70-dependent mechanism in vivo. *J. Exp. Med.* 204:1095–1106. http://dx.doi.org/10.1084/jem.20070176

Stegmann, T., F.P. Booy, and J. Wilschut. 1987. Effects of low pH on influenza virus. Activation and inactivation of the membrane fusion capacity of the hemagglutinin. *J. Biol. Chem.* 262:17744–17749.

Stegmann, T., R.W. Doms, and A. Helenius. 1989. Protein-mediated membrane fusion. *Annu. Rev. Biophys. Biophys. Chem.* 18:187–211. http://dx.doi.org/10.1146/annurev.bb.18.060189.001155

Tacken, P.J., W. Ginter, L. Berod, L.J. Cruz, B. Joosten, T. Sparwasser, C.G. Figdor, and A. Cambi. 2011. Targeting DC-SIGN via its neck region leads to prolonged antigen residence in early endosomes, delayed lysosomal degradation, and cross-presentation. *Blood.* 118:4111–4119. http://dx.doi.org/10.1182/blood-2011-04-346957

Trombetta, E.S., and I. Mellman. 2005. Cell biology of antigen processing in vitro and in vivo. *Annu. Rev. Immunol.* 23:975–1028. http://dx.doi.org/10.1146/annurev.immunol.22.012703.104538

Tsuji, T., J. Matsuzaki, M.P. Kelly, V. Ramakrishna, L. Vitale, L.Z. He, T. Keler, K. Odunsi, L.J. Old, G. Ritter, and S. Gnjatic. 2011. Antibody-targeted NY-ESO-1 to mannose receptor or DEC-205 in vitro elicits dual human CD8+ and CD4+ T cell responses with broad antigen specificity. *J. Immunol.* 186:1218–1227. http://dx.doi.org/10.4049/jimmunol.1000808

van de Ven, R., M.F. van den Hout, J.J. Lindenberg, B.J. Sluijter, P.A. van Leeuwen, S.M. Lougheed, S. Meijer, M.P. van den Tol, R.J. Scheper, and T.D. de Gruijl. 2011. Characterization of four conventional dendritic cell subsets in human skin-draining lymph nodes in relation to T-cell activation. *Blood.* 118:2502–2510. http://dx.doi.org/10.1182/blood-2011-03-344838

Villadangos, J.A., and L. Young. 2008. Antigen-presentation properties of plasmacytoid dendritic cells. *Immunity.* 29:352–361. http://dx.doi.org/10.1016/j.immuni.2008.09.002

Zelenay, S., A.M. Keller, P.G. Whitney, B.U. Schraml, S. Deddouche, N.C. Rogers, O. Schulz, D. Sancho, and C. Reis e Sousa. 2012. The dendritic cell receptor DNGR-1 controls endocytic handling of necrotic cell antigens to favor cross-priming of CTLs in virus-infected mice. *J. Clin. Invest.* 122:1615–1627. http://dx.doi.org/10.1172/JCI60644

Zhan, Y., J. Vega-Ramos, E.M. Carrington, J.A. Villadangos, A.M. Lew, and Y. Xu. 2012. The inflammatory cytokine, GM-CSF, alters the developmental outcome of murine dendritic cells. *Eur. J. Immunol.* 42:2889–2900. http://dx.doi.org/10.1002/eji.201242477

Downloaded from http://rupress.org/jem/article-pdf/210/5/1049/1748340/jem_20121251.pdf by guest on 09 February 2026